THE ASTROPHYSICAL JOURNAL, 266:105–129, 1983 March 1

PHOTOMETRIC STUDIES OF COMPOSITE STELLAR SYSTEMS. V. INFRARED PHOTOMETRY OF STAR CLUSTERS IN THE MAGELLANIC CLOUDS

S. E. PERSSON,[1] M. AARONSON,[2] JUDITH G. COHEN,[3]
JAY A. FROGEL,[4] AND K. MATTHEWS[3]

Received 1982 March 15; accepted 1982 August 24

ABSTRACT

The results of an infrared photometric study of the integrated light of 84 clusters in the Large and Small Magellanic Clouds (LMC and SMC) are presented. These clusters span nearly the complete range of cluster ages in the Clouds. In contrast to *uvgr* and *UBV* cluster colors which vary smoothly with age, the infrared colors display wide variations among the Searle, Wilkinson, and Bagnuolo groups IV–VI, i.e., in the "intermediate age" domain of ~ 1–8×10^9 yr. Very red $J-K$ and $H-K$ colors for these clusters are shown to be due to the presence of luminous ($M_{bol} < -4$) carbon stars which are absent in the youngest and oldest clusters, and which have no effect upon the visible colors. An analysis of the CO and $H-K$ data shows that on average half of the bolometric luminosity for 20 intermediate-age clusters comes from carbon stars on the asymptotic giant branch. This analysis agrees well with the recent carbon star surveys of Aaronson and Mould, Frogel and Cohen, and Lloyd-Evans.

The effects of luminous carbon stars upon the infrared colors of the parent clusters are strong enough that metal-poor, intermediate-age stellar populations may be detectable in the integrated light of more distant galaxies.

There is no difference, on average, between the clusters of the LMC and the SMC in the proportion of the light at 2 μm (or bolometrically) due to luminous carbon stars. This result is in apparent contrast to that of the Blanco *et al.* surveys of the carbon and M star populations in the general fields of the two galaxies; these surveys have revealed a sharp rise in the C/M star ratio going from the LMC to the SMC. The explanation appears to lie in the incompleteness of the Blanco *et al.* surveys for warm M stars in metal-poor populations.

Carbon stars do not appear to be present in clusters $\leq 1 \times 10^9$ yr old; the infrared colors of these young clusters are dominated by M giants and supergiants which display strong CO band absorption at 2.3 μm. This lack of carbon stars agrees with the findings of Cohen *et al.* and Richer that a true paucity of massive, luminous ($M_{bol} \leq -6$) carbon stars exists in the general fields of the Clouds. This situation is in conflict with current theories of stellar evolution on the asymptotic giant branch.

The $V-K$ colors of the youngest, i.e., 10^7–10^8 yr, clusters are compared with the single-burst model of an evolving stellar population due to Struck-Marcell and Tinsley. At a given $U-V$ the observed $V-K$ colors are up to 2 mag redder than the model predicts. The discrepancy is due to the neglect of red supergiants in the model; these luminous stars dominate the infrared colors and bolometric luminosities, and should be detectable in stellar populations like those in the arms of spiral galaxies.

The infrared colors of the oldest clusters of the Magellanic Clouds resemble those of globular clusters in our galaxy and in M31.

Subject headings: clusters: globular — clusters: open — galaxies: Magellanic Clouds — galaxies: stellar content

I. INTRODUCTION

The system of star clusters of the Magellanic Clouds differs markedly from that of our own Galaxy. The most notable differences include: (1) the apparent absence of old, metal-rich globular clusters in the Clouds (e.g., Gascoigne 1966; Searle, Wilkinson, and Bagnuolo 1980) (SWB); (2) the existence of a class of "blue

[1] Mount Wilson and Las Campanas Observatories, Carnegie Institution of Washington.
[2] Steward Observatory, University of Arizona; Visiting Astronomer, Cerro Tololo Inter-American Observatory.
[3] Division of Physics, Mathematics, and Astronomy, California Institute of Technology.
[4] Cerro Tololo Inter-American Observatory. CTIO is supported by the National Science Foundation under contract No. AST 78-27879.

populous" clusters, first discussed by Hodge (1961) which are morphologically globular in appearance, but whose color-magnitude diagrams (CMDs) show that their stellar content resembles that of associations in our Galaxy with ages in the range 10^8–10^9 years; (3) a group of "intermediate-age" clusters in the SMC identified by Gascoigne (1966), who noted their similarity to the galactic cluster NGC 2158. Finally, there exists a class of clusters in the Large Magellanic Cloud (LMC) whose color-magnitude diagrams apparently have no galactic counterparts—these include NGC 2209, 2231, and Hodge 11 (Hodge 1960). The sharp differences in the overall age distribution of populous star clusters among the three galaxies has prompted study of the cluster system from (at least) three perspectives: the nature of the clusters' stellar population, the time evolution of the metal abundance in the cluster system as a whole, and the development of integrated light techniques which can be calibrated and applied to stellar populations in more distant galaxies.

The first two approaches require well calibrated color-magnitude diagrams deep enough to reach below the turnoff of the intermediate-age and old clusters. These are difficult to obtain because of the distances of the Clouds and the considerable crowding and background problems; there is as yet no large, homogeneous set of CMDs that can be compared quantitatively with theoretical isochrones.

As an intermediate step, integrated light photometric and spectroscopic techniques have been applied to the cloud clusters and have produced valuable results. Van den Bergh and Hagen (1968) produced the first comprehensive survey of the *UBV* colors of the clusters in the Clouds. Further *UBV* work was reported by Bernard and Bigay (1974), Bernard (1975), Alcaino (1978), and Freeman and Gascoigne (1977). Danziger (1973) used an 11-color system to measure the integrated light of 20 clusters, and interpreted the differences between the clusters as due mostly to the effects of metal abundance. Recently, substantial progress in classifying the clusters through integrated light optical photometry has been made by Searle, Wilkinson, and Bagnuolo (1980, hereafter SWB). They have demonstrated that all of the clusters they observed can be arranged in a one-dimensional photometric sequence. By a comparison of the narrow-band color indices that define the sequence with those of model star clusters, they give convincing evidence that the sequence is one of age-metallicity. The one-dimensional nature of the sequence shows that age and metallicity vary smoothly *together* among the clusters. The character of the age-metallicity sequence is different from that in our Galaxy; the above-mentioned differences between the Magellanic Cloud and the Milky Way cluster systems stand out quite clearly in their classification scheme.

Integrated-light studies carried out so far have all been in the blue or visual spectral region, and consequently little emphasis has been given to those constituents of the cluster population which should dominate the red or near-infrared part of the energy distribution. This prompted us to carry out a survey of the near-infrared colors of a representative sample of clusters in both clouds. Infrared studies of globular clusters in our Galaxy (Aaronson *et al.* 1978, hereafter ACMM) and in M31 (Frogel, Persson, and Cohen 1980*b*) give a fairly clear picture of a system of old star clusters whose *VJHK* colors are one-to-one correlated with optically determined metallicities, and in which the slope of the initial mass function (IMF) is constrained to be near the Salpeter value or smaller.

Two recent developments concerning the population of late-type stars in the Clouds are relevant to the analysis of the infrared data of the Magellanic Cloud clusters. First, Blanco, Blanco, and McCarthy (1978) (BBM) pointed out a remarkably strong variation in the ratio of carbon stars to M stars found in complete surveys in going from the nuclear bulge of the Galaxy to the LMC, and from the LMC to the SMC. Second, Mould and Aaronson (1980) and Frogel, Persson, and Cohen (1980*a*) have studied individual carbon stars in the near-infrared in several Cloud clusters and have found them to be up to 2 mag brighter in M_{bol} than the than the luminosity corresponding to the termination of the first red giant branch at the helium flash. Lloyd Evans (1980) and Aaronson and Mould (1982) have photographically surveyed a large number of Cloud globular clusters for red stars; infrared photometry obtained by Aaronson and Mould (1982) and of a different sample by Frogel and Cohen (1982) have identified many new cluster carbon stars which are on the asymptotic giant branch. We show in this paper that such carbon stars are exceedingly important to the *integrated* infrared colors and total energy output of the intermediate-age clusters, while in the youngest clusters, red supergiants are important to the infrared energy output.

The data are presented in § II, and the principal observational results are listed at the end of § IIIc. In § IV the infrared colors of the intermediate-age clusters are analyzed for carbon star content and the results are compared with those from recent surveys. In § V the stellar content of the younger clusters is discussed. A summary of the conclusions of the paper is given in § VI.

II. THE DATA

a) *Observations*

The data presented in this paper were obtained on the 2.5 m du Pont and the 1 m Swope telescopes of the Las Campanas Observatory and the 0.9 m telescope of the Cerro Tololo Inter-American Observatory. Three different photometers and InSb detector systems were used; they are listed in Table 1. The HCO and CIT detector systems and the system of standard stars to which the photometry is referred have been discussed by Frogel *et al.* (1978) and by Aaronson, Frogel, and Persson (1978). The transformations which interrelate the three systems are small and well defined and have been used to place all the data presented herein on the CIT system.

TABLE 1

TELESCOPES AND EQUIPMENT

Telescope (1)	Abbr. for Tables 2 and 3 (2)	System[a] (3)	Aperture Diameter (arcsec) (4)	Abbr. for Apertures (5)	Clusters (6)
2.5 m du Pont, Las Campanas	D	CIT	12.0	12	LMC
		CIT	24.1	24	LMC
		CIT	27.8	28	LMC, SMC
		CIT	30.1	30	LMC, SMC
		CIT	35.2	35	LMC
		CIT	60.6	60	LMC, SMC
		CIT	75.0	75	LMC
1 m Swope, Las Campanas	S	HCO	28.7	29	LMC
		HCO	55.9	56	LMC
		CIT	59.2	59	LMC
0.9 m, Cerro Tololo.....	C	CIT	59.8	60	SMC
		HCO	63.6	64	LMC

[a] The HCO and CIT photometric systems are discussed in the text.

Table 1 also lists the aperture sizes used for the multiaperture measurements. For the du Pont and CTIO observations, an iris diaphragm was used, and the aperture diameters are not known to better than $\pm 1''$.

The observations made on the du Pont telescope were greatly aided by the use of a Quantex television system. For nearly all the observations the visual centering was checked by maximizing the analog signal from the infrared detector. These two methods usually gave consistent results, but in some cases the infrared centering was clearly different from the visual centering because of the presence of one or more bright stars in the measuring aperture. Bright field stars were avoided when they fell into or close to one of the two sky positions which were, in general, $100''$–$140''$ north and south of the cluster centers. The infrared data were corrected for the nonuniformity of the "beam profile" by convolving the measured beam profiles with globular cluster light distributions. In all cases, the corrections required were less than 0.05 mag. Systematic corrections for flux in the photometer reference beam from the cluster being measured were negligible in all cases.

Tables 2 and 3 list the multiaperture data. Column (2) gives a classification as globular or open cluster according to van den Bergh and Hagen (1968) or Alcaino (1978). It is an arbitrary division into clusters having a $B-V$ color greater than or less than 0.59. Columns (5) through (10) of Tables 2 and 3 list the infrared data; the $V-K$ colors are discussed separately below. Columns (11) and (12) give the number of independent measurements for the broad-band and narrow-band data, respectively. The observational 1 σ_m uncertainties are given in units of 0.01 mag in parentheses following each entry. These include statistical and photometric errors and, where appropriate, include an estimate of the error when more than one observation was made. Three significant digits have been retained for the CO and H_2O indices as a convenience in plotting and averaging the data.

Contamination of the measurements by the background, which can be large and nonuniform especially in the Bar region of the LMC, contributes further to the uncertainties. The problematical clusters are noted in column (13) of Tables 2 and 3; we have not attempted to assign larger uncertainties in these cases.

In those cases where two telescopes are listed for one particular aperture size, the individual data have been averaged, with due consideration given to the separate observational uncertainties. These repeat measurements were found to agree quite well, despite the different centering and guiding techniques used, and the generally different signal/sky aperture separations. A further indication of the agreement of the repeat measurements can be gained by looking at the colors measured through apertures which are roughly the same size; e.g., $56''$ and $60''$. In only a few cases do the individual data disagree by more than the observational uncertainties. We believe that the stochastic effects of bright stars or a nonuniform background are largely responsible for these discrepancies. For the open clusters, which tend to be highly nonuniform, and for those clusters lying close to the LMC bar, stochastic effects dominate the observational uncertainties.

b) $V-K$ Colors

The sources for the V data are van den Bergh and Hagen (1968), Bernard and Bigay (1975), Bernard (1975), van den Bergh (1981), and Alcaino (1978). In many cases, a direct $V-K$ determination was possible because the visual and infrared apertures were nearly equal in size. Where the sizes were not identical, small adjustments were made, e.g., to go from $60''$ to $61''$ or from $56''$ to $62''$. These adjustments do not add appreciable uncertainty to the measurements of clusters having smooth light distributions. Some additional $V-K$ values were obtained for aperture diameters different from those used by the above-cited authors, as follows. In an investigation of possible radial color gradients for a number of the more regular globular clusters, Searle (unpublished) has obtained multiaperture *uvgr* data on the Thuan and Gunn (1976) system for aperture sizes which bracket the infrared aperture sizes.

TABLE 2

INFRARED PHOTOMETRY OF CLUSTERS IN THE LMC

NGC	Class[a]	Tel[b]	Ap[c]	K[d]	V-K	J-K	H-K	CO	H_2O	N_{bb}[e]	N_{nb}[f]	Notes
(1)	(2)	(3)	(4)	(5)	(6)	(7)	(8)	(9)	(10)	(11)	(12)	(13)
1466	G	D	30	9.82 (3)[g]	2.48	0.68 (4)	0.14 (4)	-0.020 (2)	0.070 (2)	1	1	1
		S	56	9.51 (4)	2.14	0.49 (5)	0.06 (5)	. . .	. . .	1	0	
1644	G	D	30	11.21 (3)	. . .	0.64 (3)	0.13 (3)	0.060 (3)	0.105 (4)	2	2	
1711	O	S, D	30	9.00 (3)	1.63	0.57 (3)	0.13 (2)	0.115 (2)	0.035 (1)	2	1	
		S	56	8.72 (3)	1.43	0.49 (5)	0.10 (3)	. . .	. . .	1	0	
1751	G	D	24	9.60 (3)	. . .	1.20 (4)	0.39 (4)	0.060 (2)	0.115 (2)	1	1	
		D	30	9.40 (3)	. . .	1.21 (5)	0.40 (4)	0.045 (2)	0.060 (3)	1	1	
		D	60	8.37 (3)	3.78	1.23 (5)	0.33 (5)	. . .	. . .	1	0	
1755	O	S, D	30	8.73 (2)	1.56	0.65 (3)	0.15 (3)	0.090 (2)	0.070 (2)	2	1	
		S	56	8.39 (4)	1.60	0.50 (5)	0.14 (5)	. . .	. . .	1	0	
1767	O	S, D	30	8.32 (2)	. . .	0.86 (4)	0.19 (2)	0.250 (2)	0.030 (1)	2	1	
		S	56	7.67 (3)	. . .	0.95 (6)	0.20 (3)	. . .	. . .	1	0	
1774	O	S, D	30	8.70 (2)	2.29	0.80 (4)	0.15 (3)	0.145 (2)	0.030 (1)	2	1	
		S	56	8.56 (3)	2.22	0.71 (4)	0.17 (3)	. . .	. . .	1	0	
1783	G	D	30	9.12 (2)	2.98	0.86 (4)	0.20 (2)	0.015 (4)	0.055 (4)	1	1	2, 6, 7
		S	56	8.65 (3)	2.43	0.77 (5)	0.13 (3)	. . .	. . .	1	0	
		D	60	8.56 (4)	2.41	0.77 (5)	0.11 (5)	0.115 (2)	0.055 (3)	1	1	
1786	G	D	12	9.67 (3)	. . .	0.52 (4)	0.06 (4)	0.015 (2)	0.070 (2)	1	1	5, 15
		D	24	8.51 (3)	. . .	0.45 (4)	0.06 (4)	-0.010 (2)	0.015 (2)	1	1	
		S	29	8.35 (3)	. . .	0.54 (4)	0.12 (4)	. . .	. . .	1	0	
		S	56	8.06 (3)	. . .	0.52 (4)	0.08 (4)	. . .	. . .	1	0	
1805	O	S, D	28	7.74 (2)	3.28	0.99 (4)	0.22 (2)	. . .	. . .	2	0	
		S	56	7.64 (2)	3.02	0.88 (4)	0.20 (2)	. . .	. . .	1	0	
		D	60	7.68 (3)	2.95	0.97 (5)	0.22 (4)	0.235 (2)	0.110 (2)	1	1	
1806	G	D	24	9.09 (3)	3.37	0.96 (4)	0.23 (4)	0.100 (2)	0.110 (2)	1	1	
		S	29	9.02 (3)	3.15	. . .	. . .	. . .	. . .	1	0	
		S	56	8.44 (3)	2.90	0.91 (4)	0.25 (4)	. . .	. . .	1	0	
		D	60	8.19 (5)	3.08	1.00 (6)	0.27 (6)	0.050 (2)	0.100 (2)	1	1	
1818	O	S	29	8.20 (3)	2.08	0.84 (4)	0.16 (4)	. . .	. . .	1	0	
		S	56	7.55 (3)	2.32	0.82 (4)	0.16 (4)	. . .	. . .	1	0	
		D	60	7.49 (3)	2.36	0.86 (4)	0.16 (4)	0.185 (2)	0.070 (2)	1	1	
1831	O	D	30	10.71 (15)	1.37	0.44 (5)	0.07 (5)	0.000 (4)	0.030 (4)	1	1	11
		S	59	9.21 (3)	1.99	0.65 (4)	0.33 (4)	. . .	. . .	1	0	

TABLE 2—*Continued*

NGC	Class[a]	Tel[b]	Ap[c]	K[d]	V-K	J-K	H-K	CO	H_2O	N_{bb}[e]	N_{nb}[f]	Notes
(1)	(2)	(3)	(4)	(5)	(6)	(7)	(8)	(9)	(10)	(11)	(12)	(13)
1835	G	S	56	7.76 (3)	2.43	0.61 (6)	0.16 (3)	. . .	. . .	1	0	
		D	60	7.67 (5)	2.49	0.71 (6)	0.16 (6)	0.000 (3)	0.030 (3)	1	1	
1841	G	D	30	11.40 (4)	. . .	0.70 (2)	0.16 (2)	-0.070 (4)	-0.010 (5)	2	1	1
1846	G	D	30	9.18 (3)	. . .	1.18 (5)	0.35 (4)	0.050 (3)	0.110 (2)	1	1	1
		S	56	8.32 (3)	. . .	1.04 (5)	0.24 (4)	. . .	. . .	1	0	
		D	60	8.03 (3)	3.37	1.10 (5)	0.32 (4)	0.085 (2)	0.115 (2)	1	1	
1850	O	S	29	8.86 (4)	. . .	. . .	. . .	. . .	. . .	1	0	8
		S	56	7.90 (3)	. . .	0.60 (5)	0.15 (3)	. . .	. . .	1	0	
		D	60	7.74 (3)	1.62	0.63 (4)	0.13 (4)	0.105 (2)	0.045 (2)	1	1	
1854	O	S, D	30	9.34 (2)	. . .	0.70 (4)	0.16 (3)	0.035 (2)	0.025 (2)	2	1	
		S	56	8.66 (3)	1.80	0.54 (5)	0.16 (3)	. . .	. . .	1	0	
1855	O	S	29	9.60 (3)	. . .	. . .	. . .	. . .	. . .	1	0	
		S	56	8.67 (3)	2.10	0.58 (6)	0.12 (3)	. . .	. . .	1	0	17
1856	O	S, D	30	8.88 (4)	1.80	0.56 (4)	0.10 (4)	0.065 (1)	0.05 (1)	2	1	
		S	56	8.46 (3)	1.66	. . .	. . .	. . .	. . .	1	0	
1866	O	S	29	8.87 (4)	1.85	. . .	. . .	. . .	. . .	1	0	
		S	56	8.22 (4)	1.73	0.59 (5)	0.13 (5)	. . .	. . .	1	0	
		D	60	8.04 (3)	1.85	0.69 (4)	0.15 (4)	0.090 (2)	0.035 (2)	1	1	
1868	G	D	24	9.97 (3)	. . .	0.76 (5)	0.19 (4)	0.180 (2)	0.105 (2)	1	1	
		C	64	9.73 (4)	1.82	0.69 (5)	0.13 (4)	. . .	. . .	1	0	
1872	O	D	30	9.73 (4)	. . .	0.64 (5)	0.15 (5)	. . .	. . .	1	0	8
		D	60	9.04 (3)	2.00	0.63 (4)	0.13 (4)	0.105 (3)	0.060 (3)	1	1	
1898	G	D	24	9.84 (3)	. . .	0.75 (4)	0.14 (4)	0.000 (2)	0.015 (2)	1	1	
		D	30	9.48 (3)	. . .	0.76 (5)	0.16 (4)	0.015 (3)	0.040 (6)	1	1	
		S	56	9.21 (4)	2.29	0.80 (5)	0.13 (5)	. . .	. . .	1	0	
1916	G	S, D	30	7.89 (2)	. . .	0.89 (3)	0.24 (3)	0.090 (1)	0.110 (1)	2	1	
		S	56	7.74 (4)	. . .	0.76 (6)	0.17 (4)	. . .	. . .	1	0	
1943	O	D	30	10.84 (3)	. . .	0.58 (4)	0.12 (3)	0.035 (3)	0.025 (2)	1	1	8
1944	O	D	30	10.31 (4)	. . .	0.78 (5)	0.11 (5)	0.160 (3)	0.070 (3)	1	2	7
		S	59	9.91 (4)	. . .	0.72 (5)	0.23 (6)	. . .	. . .	1	0	
1951	O	D	30	8.60 (3)	. . .	0.84 (5)	0.20 (4)	0.140 (2)	0.075 (2)	1	1	9
		S	56	8.59 (3)	1.99	0.61 (5)	0.11 (3)	. . .	. . .	1	0	
1953	G	D	24	10.38 (3)	. . .	0.82 (5)	0.25 (4)	0.090 (3)	0.145 (2)	1	1	
		C	64	10.07 (04)	1.66	0.71 (5)	0.25 (5)	. . .	. . .	1	0	

TABLE 2—*Continued*

NGC	Class[a]	Tel[b]	Ap[c]	K[d]	V-K	J-K	H-K	CO	H_2O	N_{bb}[e]	N_{nb}[f]	Notes
(1)	(2)	(3)	(4)	(5)	(6)	(7)	(8)	(9)	(10)	(11)	(12)	(13)
1978	G	D	30	8.44 (3)	2.89	1.12 (5)	0.34 (4)	0.030 (2)	0.115 (2)	1	1	
		S	56	7.86 (4)	2.95	0.91 (5)	0.28 (5)	0.045 (2)	. . .	1	1	
		D	60	7.92 (2)	2.81	0.94 (2)	0.25 (1)	0.040 (1)	0.100 (1)	2	2	
1984	O	D	30	8.27 (3)	. . .	0.78 (5)	0.27 (4)	0.060 (2)	0.105 (2)	1	1	
		S	56	8.16 (4)	. . .	0.62 (6)	0.21 (6)	. . .	. . .	1	0	
1986	O	D	30	9.85 (10)	2.00	0.83 (2)	0.17 (1)	0.135 (1)	0.090 (1)	3	3	1
1987	G	D	24	10.00 (3)	3.03	0.88 (5)	0.19 (4)	0.190 (2)	0.070 (2)	1	1	
		D	30	9.87 (4)	2.90	0.83 (5)	0.15 (5)	0.170 (2)	. . .	1	1	
		D	60	9.01 (3)	3.13	1.08 (5)	0.37 (4)	. . .	. . .	1	0	
		C	64	9.06 (3)	3.03	1.06 (4)	0.30 (4)	. . .	. . .	1	0	
1994	O	S	14	7.26 (4)	. . .	. . .	. . .	. . .	. . .	1	0	
		S, D	30	7.04 (2)	. . .	0.99 (2)	0.30 (2)	0.140 (3)	0.130 (3)	2	1	6
		S	56	7.01 (4)	. . .	0.94 (6)	0.30 (6)	0.145 (2)	. . .	1	1	
2002	O	S, D	30	6.74 (2)	. . .	0.93 (2)	0.20 (1)	0.240 (2)	0.075 (3)	2	1	
		S	56	6.73 (2)	. . .	0.87 (6)	0.18 (6)	0.240 (2)	. . .	1	1	
2004	O	S, D	30	7.19 (2)	2.95	0.95 (2)	0.20 (2)	0.225 (3)	0.080 (3)	2	1	2, 6
		D	35	7.22 (3)	2.85	0.93 (4)	0.18 (4)	0.240 (2)	0.075 (2)	1	1	
		S	56	7.15 (3)	2.66	0.87 (5)	0.17 (5)	0.220 (2)	. . .	1	1	
		D	75	6.89 (3)	. . .	0.95 (4)	0.21 (4)	0.240 (2)	0.070 (2)	1	1	
2011	O	D	30	8.05 (3)	. . .	0.91 (5)	0.23 (4)	0.235 (2)	0.085 (2)	1	1	
		S	56	7.85 (3)	. . .	0.92 (6)	0.17 (4)	. . .	. . .	1	0	
2019	G	D	24	9.06 (3)	2.33	0.61 (4)	0.09 (4)	0.000 (2)	0.010 (2)	1	1	3, 1
		S	56	8.55 (3)	2.41	0.59 (6)	0.07 (4)	. . .	. . .	1	0	
2041	O	D	30	8.83 (3)	1.96	0.70 (5)	0.14 (4)	0.080 (2)	0.045 (2)	1	1	
		S	56	8.62 (3)	1.77	0.56 (5)	0.10 (4)	. . .	. . .	1	0	
2058	O	D	30	9.37 (10)	3.07	0.73 (5)	0.15 (4)	0.165 (2)	0.070 (2)	0	1	3
		S	59	9.03 (3)	2.83	0.66 (4)	0.09 (4)	. . .	. . .	1	0	
2065	O	D	30	10.62 (15)	. . .	0.57 (5)	0.06 (4)	0.040 (3)	0.115 (3)	1	1	10
		S	59	9.98 (4)	1.27	0.48 (5)	0.02 (5)	. . .	. . .	1	0	
2070	O	S	56	7.29 (3)	. . .	0.35 (4)	0.22 (4)	0.000 (3)	. . .	1	1	8
2100	O	S, D	30	7.76 (15)	2.61	0.90 (7)	0.21 (7)	0.225 (3)	0.215 (3)	2	1	2, 6
		S	56	6.98 (3)	2.67	0.97 (5)	0.28 (4)	0.160 (2)	. . .	1	1	
		D	60	6.65 (3)	2.95	1.03 (5)	0.27 (4)	0.240 (2)	0.095 (2)	1	1	
2107	O	D	30	9.53 (3)	2.62	0.99 (5)	0.25 (4)	0.120 (2)	0.090 (2)	1	1	
		D	60	9.21 (4)	2.30	0.82 (5)	0.21 (5)	. . .	. . .	1	0	3

TABLE 2—*Continued*

NGC	Class[a]	Tel[b]	Ap[c]	K[d]	V-K	J-K	H-K	CO	H_2O	N_{bb}[e]	N_{nb}[f]	Notes
(1)	(2)	(3)	(4)	(5)	(6)	(7)	(8)	(9)	(10)	(11)	(12)	(13)
2108	G	D	24	9.66 (3)	. . .	1.38 (5)	0.58 (4)	-0.010 (2)	0.185 (3)	1	1	
		C	64	9.27 (4)	3.04	1.18 (4)	0.46 (4)	. . .	. . .	1	0	
2121	G	D	30	10.24 (15)	. . .	1.01 (5)	0.20 (4)	0.110 (2)	0.155 (5)	2	2	1, 7
		D	60	8.99 (3)	3.40	1.14 (4)	0.40 (4)	. . .	. . .	1	0	
2134	O	D	24	9.85 (3)	1.96	0.67 (4)	0.12 (4)	0.105 (2)	0.040 (3)	1	1	
		C	64	9.36 (3)	1.65	0.54 (4)	0.07 (4)	. . .	. . .	1	0	
2136	O	D	24	9.15 (3)	. . .	0.74 (4)	0.15 (4)	0.100 (2)	0.070 (2)	1	1	
		S	29	9.08 (3)	. . .	. . .	. . .	. . .	. . .	1	0	
		S	56	8.69 (3)	1.88	0.59 (5)	0.12 (4)	. . .	. . .	1	0	
2154	G	D	24	9.77 (3)	. . .	1.31 (5)	0.45 (4)	0.025 (2)	0.140 (2)	1	1	
		C	64	8.88 (3)	3.23	1.25 (4)	0.49 (4)	. . .	. . .	1	0	
2155	G	D	30	10.78 (4)	. . .	0.85 (5)	0.16 (4)	0.095 (3)	0.015 (3)	1	1	4
2156	O	D	30	10.99 (4)	. . .	0.24 (4)	0.02 (2)	-0.025 (7)	0.015 (4)	2	1	
2157	O	D	24	9.26 (3)	1.71	0.63 (4)	0.12 (4)	0.055 (2)	0.030 (2)	1	1	
		S	29	9.18 (3)	1.52	. . .	. . .	. . .	. . .	1	0	
		S	56	8.45 (3)	1.74	0.67 (5)	0.16 (4)	. . .	. . .	1	0	
2159	O	D	30	10.86 (4)	. . .	0.52 (5)	0.07 (5)	0.030 (6)	0.045 (6)	1	1	
		S	59	9.99 (10)	. . .	0.46 (6)	0.01 (7)	. . .	. . .	1	0	7
2162	G	D	30	10.39 (3)	. . .	0.99 (4)	0.21 (4)	0.130 (2)	0.100 (3)	1	1	
2164	O	D	30	9.70 (3)	3.08	0.46 (5)	0.09 (4)	0.055 (2)	0.050 (3)	1	1	
		S	56	9.31 (3)	3.07	0.40 (5)	0.08 (4)	. . .	. . .	1	0	
2172	O	S	59	10.64 (6)	. . .	0.48 (7)	0.12 (7)	. . .	. . .	1	0	7
2173	G	D	30	9.90 (3)	. . .	1.08 (5)	0.25 (4)	0.165 (2)	0.130 (2)	1	1	
2209	G	D	30	10.04 (3)	. . .	1.72 (2)	0.67 (2)	-0.050 (3)	0.275 (4)	2	1	14
2210	G	D	24	9.22 (3)	2.30	0.62 (5)	0.09 (4)	0.005 (2)	0.060 (2)	1	1	
		S	56	8.91 (6)	2.07	0.56 (6)	0.10 (4)	. . .	. . .	1	0	
2213	G	D	24	9.79 (3)	. . .	1.13 (5)	0.37 (4)	-0.010 (2)	0.085 (3)	1	1	
		C	64	9.37 (4)	3.00	1.12 (4)	0.37 (5)	. . .	. . .	1	0	

TABLE 2—*Continued*

NGC	Class[a]	Tel[b]	Ap[c]	K[d]	V-K	J-K	H-K	CO	H_2O	N_{bb}[e]	N_{nb}[f]	Notes
(1)	(2)	(3)	(4)	(5)	(6)	(7)	(8)	(9)	(10)	(11)	(12)	(13)
2214	O	D	24	10.09 (3)	1.67	0.76 (4)	0.16 (4)	0.170 (2)	0.050 (2)	1	1	12
		S	56	9.07 (4)	1.91	0.76 (8)	0.19 (6)	. . .	. . .	1	0	
2231	G	D	30	10.37 (3)	. . .	1.41 (4)	0.42 (3)	0.060 (5)	0.240 (5)	1	1	
2257	G	D	30	12.53 (4)	. . .	0.60 (5)	0.10 (5)	. . .	. . .	1	0	1
Hodge 11	G	D	30	10.78 (4)	. . .	0.63 (5)	0.13 (5)	-0.010 (3)	0.055 (3)	1	1	

NOTES TO TABLES 2 AND 3

[1] Object is very extended and difficult to center. Centering probably affects growth curve at K.
[2] Extended with obvious bright stars in field. Likely that the optical and infrared maxima are not coincident. Growth curves and $V-K$ colors are therefore uncertain.
[3] Object is difficult to center.
[4] Object is sparse and difficult to center because of discrete stars.
[5] A single bright star is included in the larger apertures. Affects colors and growth curves.
[6] Many bright stars in the aperture.
[7] Possibly nonphotometric at the 0.05 mag level.
[8] Object is in or associated with emission nebulosity. Omitted from plots and analysis.
[9] Object is very concentrated and structured. Discrepant colors could be due to centering or variability of one dominant star. An old measurement gave $K = 9.25$ in a 28″.7 diameter aperture.
[10] Exact iris diaphragm aperture diameter uncertain. Corrected brighter by 0.1 mag.
[11] Large color change between different apertures possibly due to red star(s) included in the larger aperture.
[12] Centered on west clump of cluster.
[13] Bright star 5″ south of center; centering affected.
[14] Infrared data and centering affected by carbon stars W46 and W50 (Walker 1971). See § IVc.
[15] Star superposed. See van den Bergh and Hagen 1968 and notes to Table 4 for $(V-K)_0$.

[a] O = open; G = globular; from van den Bergh and Hagen 1968 and Alcaino 1978.
[b] See code in Table 1.
[c] Exact aperture diameters given in Table 1.
[d] Magnitudes, colors, and indices not corrected for reddening.
[e] Number of separate broad-band JHK measurements.
[f] Number of separate narrow-band CO and H_2O measurements.
[g] 1 σ_m errors are given in parentheses in hundredths of a magnitude.

TABLE 3

INFRARED PHOTOMETRY OF CLUSTERS IN THE SMC

NGC	Class[a]	Tel[b]	Ap[c]	K[d]	V-K	J-K	H-K	CO	H_2O	N_{bb}[e]	N_{nb}[f]	Notes
(1)	(2)	(3)	(4)	(5)	(6)	(7)	(8)	(9)	(10)	(11)	(12)	(13)
121	G	D	30	9.28 (3)	. . .	0.78 (5)	0.15 (4)	0.045 (2)	0.060 (3)	1	1	
			60	8.83 (2)	2.44	0.74 (2)	0.13 (2)	0.035 (2)	0.110 (2)	2	2	
152	G	D	30	10.97 (3)	. . .	1.02 (5)	0.24 (4)	0.070 (6)	-0.035 (6)	1	1	6
		C	60	9.60 (2)	3.52	1.11 (2)	0.39 (2)	. . .	. . .	1	0	
220	O	D	30	11.68 (4)	. . .	0.53 (5)	0.15 (5)	. . .	. . .	1	0	4
222	O	D	30	12.45 (5)	. . .	0.48 (6)	0.12 (5)	. . .	. . .	1	0	4
242	O	D	30	11.34 (4)	. . .	0.64 (5)	0.19 (5)	0.100 (4)	0.070 (5)	1	2	4
256	O	D	30	10.68 (2)	. . .	0.65 (2)	0.11 (2)	0.025 (2)	-0.010 (4)	2	2	
		D	60	10.66 (4)	1.71	0.66 (5)	0.05 (5)	. . .	. . .	1	0	
265	O	D	30	11.46 (5)	. . .	0.46 (6)	0.05 (5)	0.065 (5)	-0.010 (6)	1	1	5
		D	60	10.28 (5)	1.87	0.77 (6)	0.15 (5)	. . .	. . .	1	0	5
269	O	D	30	10.46 (10)	. . .	0.89 (5)	0.17 (4)	. . .	. . .	1	0	3, 13
		D	60	10.42 (4)	1.22	0.76 (5)	0.17 (5)	. . .	. . .	1	0	3, 13
299	O	D	30	8.82 (3)	. . .	0.86 (5)	0.14 (4)	0.195 (2)	0.105 (3)	1	1	
		D	60	8.67 (2)	3.47	0.86 (2)	0.14 (2)	. . .	. . .	2	1	
330	O	D	28	8.37 (7)	1.83	0.73 (5)	0.12 (5)	. . .	. . .	2	0	2, 3
		D	30	8.14 (3)	1.98	0.82 (4)	0.18 (4)	0.105 (2)	0.040 (2)	1	1	2, 3
		D	60	7.69 (2)	1.94	0.78 (2)	0.13 (2)	0.150 (1)	0.070 (1)	2	2	
339	G	C	60	10.59 (3)	2.40	0.59 (4)	0.08 (4)	. . .	. . .	1	0	
346	O	D	30	10.79 (4)	. . .	0.66 (5)	0.51 (4)	-0.215 (3)	. . .	1	1	8
361	G	C	60	9.78 (2)	. . .	0.71 (3)	0.16 (3)	. . .	. . .	1	0	15
411	G	D	30	10.23 (3)	. . .	1.02 (5)	0.27 (4)	0.025 (3)	. . .	1	1	1
416	G	D	30	9.53 (4)	. . .	0.69 (5)	0.16 (4)	0.010 (2)	0.030 (2)	1	1	
		C	60	9.01 (2)	2.45	0.66 (2)	0.14 (2)	. . .	. . .	1	0	
419	G	D	30	8.32 (3)	3.08	1.14 (4)	0.37 (4)	-0.020 (2)	0.115 (2)	1	1	3
		D	60	7.69 (2)	2.97	1.11 (2)	0.34 (1)	0.035 (1)	0.145 (1)	2	2	
458	O	D	30	11.39 (4)	1.01	0.47 (5)	0.12 (5)	0.020 (5)	-0.020 (5)	1	2	
L 56	O	D	30	10.42 (3)	1.20	0.53 (5)	0.09 (4)	0.070 (4)	. . .	1	1	7
L 72	O	D	30	8.91 (3)	2.14	0.68 (5)	0.11 (4)	0.120 (2)	0.050 (2)	1	1	7
K 3	G	D	30	11.26 (3)	. . .	0.55 (4)	0.07 (5)	-0.050 (5)	0.065 (7)	1	1	
		C	60	9.77 (3)	2.31	0.65 (3)	0.11 (3)	. . .	. . .	1	0	

TABLE 4

INFRARED COLORS FOR LMC CLUSTERS

NGC	Type[a]	t	E(B-V)[b]	$(V-K)_o$	$(J-K)_o$	$(H-K)_o$	CO	H_2O	NOTES
(1)	(2)	(3)	(4)	(5)	(6)	(7)	(8)	(9)	(10)
1466	VII	274	0.07	2.12	0.55 (9)[c]	0.09 (4)	-0.020	0.065	
1644	V	224	0.07	. . .	0.60	0.12	0.060 (3)	0.100 (4)	
1711	II	122	0.16	1.09	0.44	0.09	0.120	0.025	
1751	V	224	0.12	3.45	1.14	0.34	0.055	0.085	1, 2
1755	II-III	142	0.12	1.25	0.51 (6)	0.12	0.095	0.065	
1767[d]	. . .	. . .	0.15	2.26	0.81 (4)	0.16	0.255	0.020	
1774	II	113	0.10	1.98	0.70 (4)	0.14	0.150	0.025	
1783[e]	V	225	0.10	2.33	0.74	0.13	0.065 (5)	0.050 (3)	2
1786	. . .	. . .	0.12	2.20	0.44	0.05	0.005	0.035 (3)	
1805	. . .	. . .	0.10	2.80	0.89	0.19	0.240	0.105	
1806	V	231	0.12	2.79	0.89	0.22	0.080 (3)	0.100	1, 2
1818	I	67	0.10	1.97	0.78	0.14	0.190	0.065	
1831	V	211	0.10	1.40	0.48 (10)	0.18 (13)	0.005 (4)	0.025 (4)	2
1835	VII	272	0.12	2.13	0.59 (5)	0.13	0.005 (3)	0.025 (3)	
1841	VII	292	0.07	2.29	0.66	0.15	-0.070 (4)	-0.015 (5)	3
1846	V	219	0.10	3.09	1.05 (4)	0.28	0.075	0.105	1, 2
1850	. . .	. . .	0.15	1.20	0.54	0.11	0.110	0.035	
1854	II	134	0.13	1.44	0.55 (8)	0.13	0.040	0.020	
1855	. . .	. . .	0.12	1.84 (20)	0.51 (6)	0.09	. . .	. . .	
1856	IV	191	0.24	1.06	0.43 (4)	0.05 (4)	0.070	0.040	
1866	III	169	0.10	1.53	0.58 (5)	0.12	0.095	0.030	3
1868	. . .	. . .	0.07	1.63	0.69	0.15	0.180	0.100	
1872	III-IV	178	0.13	1.64	0.56	0.11	0.100 (3)	0.055 (3)	
1898	. . .	. . .	0.09	2.04	0.72	0.12	0.010	0.015	
1916[d]	. . .	. . .	0.16	2.12	0.74 (6)	0.18	0.095	0.100	2
1943	III	150	0.18	. . .	0.48 (4)	0.08	0.040 (3)	0.015	
1944	. . .	. . .	0.07	. . .	0.71	0.16 (6)	0.160 (3)	0.065 (3)	
1951	. . .	. . .	0.10	1.71	0.67 (12)	0.14 (5)	0.145	0.070	
1953	. . .	. . .	0.12	1.33	0.70 (5)	0.22	0.095 (3)	0.140	
1978	VI	239	0.10	2.58	0.93 (7)	0.27	0.045	0.100	1, 2
1984[g]	. . .	. . .	0.15	1.20	0.62 (8)	0.21	0.065	0.095	
1986	II	135	0.18	1.50	0.73	0.13	0.140	0.080	
1987[d]	IV	193	0.12	2.69	0.89 (6)	0.22 (5)	0.185	0.075	1, 2
1994[d]	. . .	. . .	0.14	2.42	0.89	0.27	0.150	0.120 (3)	1, 3
2002[d]	. . .	. . .	0.12	3.06	0.84	0.17	0.245	0.070 (3)	
2004[d]	I	11	0.06	2.65	0.90	0.18	0.230	0.075	
2011	. . .	. . .	0.08	2.43	0.87 (4)	0.18	0.235	0.080	
2019	VII	265	0.18	1.87	0.50	0.04	0.005	0.000	3
2041	III	152	0.05	1.73	0.60 (7)	0.11	0.080	0.040	
2058	III	162	0.18	2.45	0.60	0.08	0.170	0.060	3
2065	III	165	0.18	0.77	0.43 (4)	0.00	0.045 (3)	0.105 (3)	
2070	. . .	. . .	0.18	. . .	0.25 (4)	0.18 (4)	0.005 (3)	. . .	
2100	I	50	0.24	2.07	0.84 (4)	0.22	0.215 (3)	0.150 (5)	1
2107	IV	198	0.19	1.93	0.80 (8)	0.20	0.125	0.080	3
2108	. . .	. . .	0.18	2.54	1.18 (10)	0.48 (6)	-0.015	0.175 (3)	1, 2
2121	VI	247	0.10	3.12	1.02 (7)	0.28	0.115	0.150 (5)	1, 3
2134	IV	193	0.10	1.53	0.55 (6)	0.08	0.110	0.035 (3)	
2136	III	154	0.10	1.60	0.60 (8)	0.11	0.105	0.065	3
2154	V	229	0.10	2.95	1.22	0.45	0.030	0.135	1, 2
2155	VI	246	0.10	. . .	0.79 (5)	0.14 (4)	0.100 (3)	0.010 (3)	
2156	. . .	. . .	0.10	. . .	0.18 (4)	0.00	-0.020 (7)	0.010 (4)	
2157	. . .	. . .	0.10	1.38	0.59	0.12	0.060	0.025	
2159	. . .	. . .	0.10	. . .	0.43 (4)	0.03 (4)	0.035 (6)	0.040 (6)	
2162	V	222	0.07	. . .	0.95 (4)	0.20 (4)	0.130	0.095 (3)	3
2164	III	160	0.10	0.80	0.37	0.07	0.060	0.045 (3)	
2172	. . .	. . .	0.10	. . .	0.42 (7)	0.10 (7)	. . .	. . .	
2173	V-VI	233	0.07	2.99	1.04 (5)	0.24 (4)	0.165	0.125	1, 3
2209	III-IV	178	0.07	. . .	1.68	0.66	-0.050 (3)	0.270 (4)	1, 2
2210	VII	277	0.10	1.90	0.53 (4)	0.07	0.010	0.055	
2213	V-VI	228	0.10	2.72	1.07	0.35	-0.005	0.080 (3)	1, 2
2214	II	140	0.10	1.51	0.70	0.16	0.170	0.045	3
2231	V	223	0.10	. . .	1.35 (4)	0.40	0.065 (5)	0.235 (5)	1, 2
2257	VII	285	0.07	. . .	0.56 (5)	0.09 (5)	. . .	. . .	3
Hodge 11	VII	283	0.10	. . .	0.57 (5)	0.11 (5)	-0.005 (3)	0.050 (3)	3

Searle has kindly given us access to his original data from which we constructed growth curves for the g filter ($\lambda \sim 4910$ Å; $\Delta\lambda \sim 700$ Å). These growth curves were first compared with all the available V growth curves; the agreement was excellent, with the discrepancies rarely exceeding 5%. The g growth curves were then used to obtain V magnitudes within the aperture sizes used for the infrared measurements. Use of the g growth curves introduces little additional error into the $V-K$ colors, due either to the difference in effective wavelength between g and V, or to stochastic effects, which for these particular clusters were known beforehand to be small. For many of the clusters the stochastic effects (discussed above) dominate the uncertainties and we have therefore assigned a (conservative) nominal uncertainty of ± 0.15 mag to all the $V-K$ values. All of the multiaperture $V-K$ values are listed in column (6) of Tables 2 and 3.

c) *Averaged Colors*

In order to discuss the basic observational results, infrared colors and indices which represent each cluster as a whole are useful. In some cases such values are rather artificial, as there are differences in the colors and indices from one aperture to another. We have adopted the view that the separate measurements should be simply averaged, with a roughly linear weighting appropriate to the quoted errors. It could be argued that the best color is that measured using the largest aperture, but the irregular nature of the background, together with the magnitudes of the individual observational uncertainties, argue weakly for a simple averaging.

Tables 4 and 5 give the final adopted colors and uncertainties, which now include the dispersions in the multiaperture data. Column (4) of Table 4 lists the reddening values used to correct the infrared colors of each cluster on an individual basis. The procedures used to establish the $E(B-V)$ values are the same as those used to correct the infrared colors of individual late-type stars in clusters and fields of the Magellanic Clouds (Cohen *et al.* 1981, hereafter CFPE; Frogel and Cohen 1982).[5]

[5] The adopted reddening values are rather large compared to those conventionally used (e.g., van den Bergh and Hagen 1968), and the present authors do not agree on which are to be preferred. The conclusions of this paper are little affected by the choice of reddening values.

We shall also make use of published $U-B$ and $B-V$ colors. The sources are listed above; in general, the UBV data for clusters observed by more than one author agree very well, and where multiaperture data exist, we have taken averages to correspond to the averages over the multiaperture infrared data. In plotting the UBV data we have corrected the colors according to the values of $E(B-V)$ listed in Tables 4 and 5.

d) *The SWB Classification Parameter*

The observations and analysis by SWB of the *uvgr* colors of 61 star clusters in the Magellanic Clouds have produced a useful classification scheme. From linear combinations of the *uvgr* colors, SWB derived two reddening-free parameters Q_{ugr} and Q_{vgr} (see also Zinn 1980), which measure the depression of the flux at u and v below a continuum in the g and r region. Figure 1 shows a schematic of the cluster distribution taken from SWB. The morphology of the Q-Q diagram for stars and composite systems has been fully discussed by SWB. Briefly, Q_{vgr} is sensitive mostly to metal line absorption while Q_{ugr} is strongly affected by Balmer continuum absorption as well as metal line absorption. These dependences cause the Q's to be sensitive to both the age and metallicity of composite systems; in the upper left of Figure 1 the Q's are sensitive mostly to age, while at the other end of the sequence they are sensitive mostly to metal abundance. SWB have defined seven zones, with zone I containing the youngest clusters and zone VII the oldest. Hodge's (1960, 1961) division into "red" and "young populous" groups follows the SWB scheme closely, with the "red" clusters falling only in groups IV–VII, and the "young populous" clusters only in groups I–IV. Metal-poor globular clusters in the Galaxy lie in zone VII, and more metal-rich Galactic globular clusters lie down and to the right of zone VI where no Cloud clusters are found. Through comparison of the locations of the clusters with such CMDs as exist, SWB have given convincing evidence that the distance *along* the sequence is due mostly to *age* up to the V–VI boundary.

We have found it convenient, purely for purposes of plotting the data, to further subdivide the SWB classification. We first drew a ridge line (by eye) through the SWB distribution and then assumed that each cluster fell off the ridge line because of observational error alone.

NOTES TO TABLE 4

[a] Types from Searle, Wilkinson, and Bagnuolo 1980.

[b] Reddening values for individual clusters derived as discussed in CFPE. Colors in succeeding columns are corrected for reddening.

[c] 1 σ_m errors are given in parentheses in hundredths of a magnitude. No entry means the error is less than or equal to 0.15 mag for $(V-K)_0$, 0.03 mag for $(J-K)_0$ and $(H-K)_0$, and 0.02 mag for CO and H_2O.

[d] NGC 1767, 1916, 1994, 2002, 2011: $V-K$ found by interpolation between 2 K magnitudes to match a single V point in a 44″ or 45″ diameter aperture.

[e] NGC 1786 has a star superposed. The data of van den Bergh and Hagen 1968 were used to estimate that for this star: $V-K = 1.44$ and $K = 9.52$. Correcting for the star in the 56″ aperture gives K (56″ less star) = 8.39 and $V-K = 2.53$.

[f] NGC 1855: Not enough data exist to derive a reliable $V-K$. A linear extrapolation of the K growth curve gives for a 72″ aperture $K = 8.15$, and hence $V-K = 2.06$. If the growth curve turns over, then $V-K < 2.06$.

[g] NGC 1984: $V-K$ found by extrapolation of the K growth curve to a 72″ aperture.

[1] Member of the "IR-enhanced" group.

[2] Carbon stars searched for and found in surveys.

[3] Carbon stars searched for but *not* found in surveys.

TABLE 5

INFRARED COLORS FOR SMC CLUSTERS

NGC (1)	Type[a] (2)	t (3)	$(V-K)_0$[b] (4)	$(J-K)_0$ (5)	$(H-K)_0$ (6)	CO (7)	H_2O (8)	Notes (9)
121	VII	259	2.25	0.71	0.13	0.040	0.080 (3)	2
152	IV	200	3.33	1.03 (4)[c]	0.33 (5)	0.070 (6)	−0.040 (6)	1, 2
220	III	161	...	0.49 (5)	0.14 (5)	...	...	
222	II–III	146	...	0.44 (6)	0.11 (5)	...	...	
242	II	139	...	0.60 (5)	0.18 (5)	0.100 (4)	0.065 (5)	
256	II	138	1.52	0.61	0.08	0.025	−0.015 (4)	
265	III	158	1.68	0.58 (16)	0.09 (5)	0.065 (5)	−0.015 (6)	3
269	III–IV	180	1.03	0.78 (6)	0.16	...	...	3
299	I	9	3.28	0.82	0.13	0.195	0.100 (3)	3
330	I	80	1.73	0.74	0.13	0.130	0.055	
339	VII	271	2.21	0.55 (4)	0.07 (4)	...	...	3
346	...	...	...	0.62 (5)	0.50 (4)	−0.215 (3)	...	
361[d]	...	...	2.56	0.67	0.15	...	...	3
411	V–VI	227	...	0.98 (5)	0.26 (4)	0.025 (3)	...	1, 2
416	VI	246	2.26	0.63	0.14	0.010	0.025	3
419	V	217	2.84	1.08	0.34	0.020	0.130	1, 2
458	III	169	0.82	0.43 (5)	0.11 (5)	0.020 (5)	−0.025 (5)	
L56	II	113	1.01	0.49 (5)	0.08 (4)	0.070 (4)	...	
L72	I	85	1.95	0.64 (5)	0.10 (4)	0.120	0.045	
K3	...	...	2.12	0.56 (5)	0.09	−0.050 (5)	0.060 (7)	2

[a] See Table 4.

[b] Colors and indices corrected for reddening corresponding to $E(B-V) = 0.07$: $E(V-K) = 0.19$; $E(J-K) = 0.04$; $E(H-K) = 0.01$; $E(\mathrm{CO}) = 0.0$; $E(H_2O) = 0.005$.

[c] See Table 4.

[d] NGC 361 has a star superposed. The data of van den Bergh and Hagen 1968 were used to estimate that for this star $V-K = 2.43$ and $K = 11.50$. Correcting for the star in the 60″ aperture gives K (60″ less star) = 10.03 and $V-K = 2.75$.

[1] Member of the "IR-enhanced" group.

[2] Carbon stars searched for and found in surveys.

[3] Carbon stars searched for but *not* found in surveys.

The distances t along the sequence, measured in arbitrary units as illustrated in Figure 1, are given in Tables 4 and 5 along with the SWB group classification. As explained by SWB, the distance t along the sequence is some smoothly increasing function of the age of the population up to group IV in Figure 1, where the metal abundance begins to affect both Q_{ugr} and Q_{vgr}. As shown by SWB, the deblanketing vectors in the group V region are nearly orthogonal to the cluster ridge line, and thus t continues to increase smoothly with age up to the boundary of groups V and VI. In lieu of more accurate age data for the clusters, we shall use the t parameter as a convenience in displaying our data. The errors in t, due to observational scatter about the ridge line, we estimate to be no more than ± 20 units, which is $\pm 7\%$ of the total range in t, of 0 to 300.

III. RESULTS

a) *Infrared Colors and Indices as Functions of Age*

In Figures 2 and 3 the averaged infrared colors and indices for the clusters in Tables 4 and 5 are plotted against the age parameter t. Open and closed circles correspond to van den Bergh and Hagen's division into "open" and "globular" clusters (which is based on $B-V$ color, not morphology). For purposes of orientation, NGC 2209 is labeled on each of the separate plots of Figures 2 and 3. Gascoigne *et al.* (1976) assigned an age of 8×10^8 years to this cluster while Rabin (1980) obtains $1.5–2.5 \times 10^9$ years. Both estimates are consistent with its location in the Q-Q diagram as a group III–IV cluster.

The first result, common to the $J-K$, $H-K$, and $V-K$ colors, is that an abrupt transition occurs in the $t = 200–250$ region, which corresponds to SWB groups IV and V. The scatter in $J-K$ and $H-K$ at a given t in groups IV, V, and VI far exceeds the observational uncertainties and is significantly greater than the scatter in the I–III and VII groups. In $V-K$ the distribution of points displays a discontinuity, with a large amount of scatter superposed.

In $B-V$ versus t the division into red and blue groups pointed out by van den Bergh and Hagen (1968) and discussed by Gascoigne (1980) occurs at the same point, $t \sim 200$, that the scatter in the infrared colors sets in. The relatively smooth variations in the UBV and $uvgr$ colors imply that the *visual* energy distributions of the clusters change smoothly and continuously, as would be

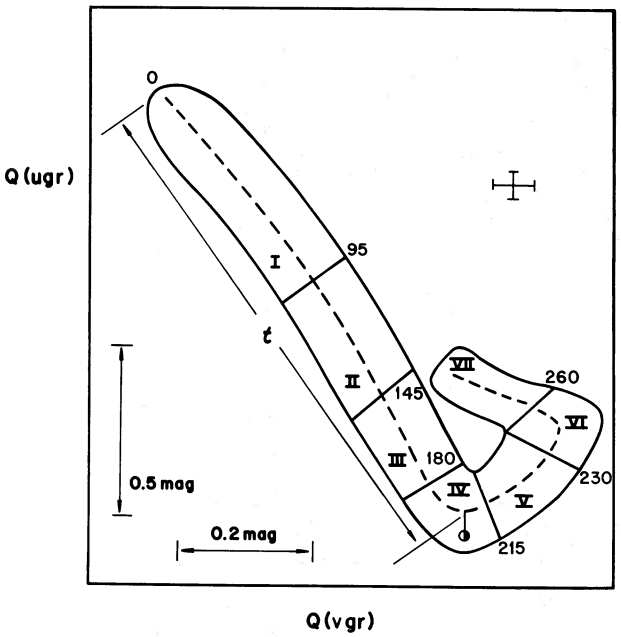

FIG. 1.—Schematic Q-Q diagram adapted from the work of SWB. The Q's, which are sensitive to the age and metal abundance of integrated light systems, are explained fully by SWB, and are described briefly in the text. The region encloses all of the SMC and LMC clusters measured by SWB. Their subdivision into seven groups, and our further subdivision into values to t for each cluster, are indicated. The values of t at each group boundary are given. The error bar is SWB's average $\pm 1\ \sigma_m$ uncertainty. Globular clusters of the Milky Way extend through the group VII and VI regions and down and to the right off the plot; see Zinn (1980).

expected from the fact that visual colors and indices are determined largely by the well-populated sequences of the H-R diagram. In the near-infrared, on the other hand, we are presumably measuring relatively rare components of the stellar population whose contribution can undergo large stochastic variations—red giant and asymptotic giant branch stars. In particular, the $H-K$ color is so well confined to the infrared part of the energy distribution that the only possible explanation for its variations lies with strongly varying relative contributions from the very latest-type stars in the clusters. We emphasize that little or none of the scatter seen in the infrared colors at a given t is reflected in the Q-Q diagram or in the UBV colors. In fact, one of SWB's principal results is that the dispersion about the ridge line of the Q-Q diagram could be atrributed solely to observational uncertainties. Figure 2 shows that this is not at all the case for the $J-K$, $H-K$, and $V-K$ colors.

Figure 3 plots the CO and H_2O indices against t. There is weak evidence for a bump or an increase in scatter near $t = 200$ in the H_2O index, but no shift or sharply increased amount of scatter in the CO index.

b) *Principal Contributors to the Infrared Light of the Cloud Clusters*

We now discuss the composition of the cluster light, by comparing the infrared colors and narrow band indices of the clusters with those of stars that can conceivably contribute strongly. Figures 4, 5, 6, and 7 present several two-color diagrams plotted from the data in Tables 4 and 5. Included on the plots are the regions occupied by various kinds of late-type stars, globular clusters, and galaxies. The sources for these data can be

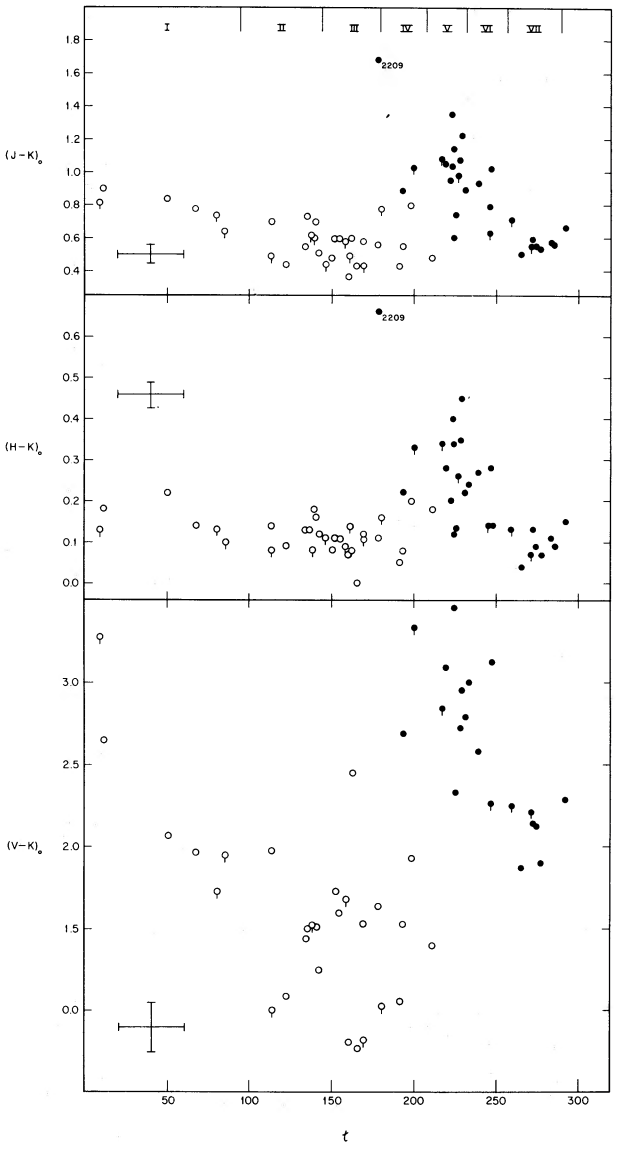

FIG. 2.—Reddening-corrected broad-band colors for LMC and SMC clusters (data from Tables 4 and 5) are plotted against the age parameter t defined in the text and in Fig. 1. The SWB group boundaries are also shown. Open and closed symbols correspond to van den Bergh and Hagen's (1968) division into "open" and "globular" clusters. Flagged symbols are SMC clusters. Typical $\pm 1\ \sigma_m$ error bars are shown for each color or index.

NGC 2070 (30 Doradus cluster) and NGC 346 are not plotted in any of the figures or discussed further. Their infrared colors are strongly affected by free-free emission from their associated H II regions.

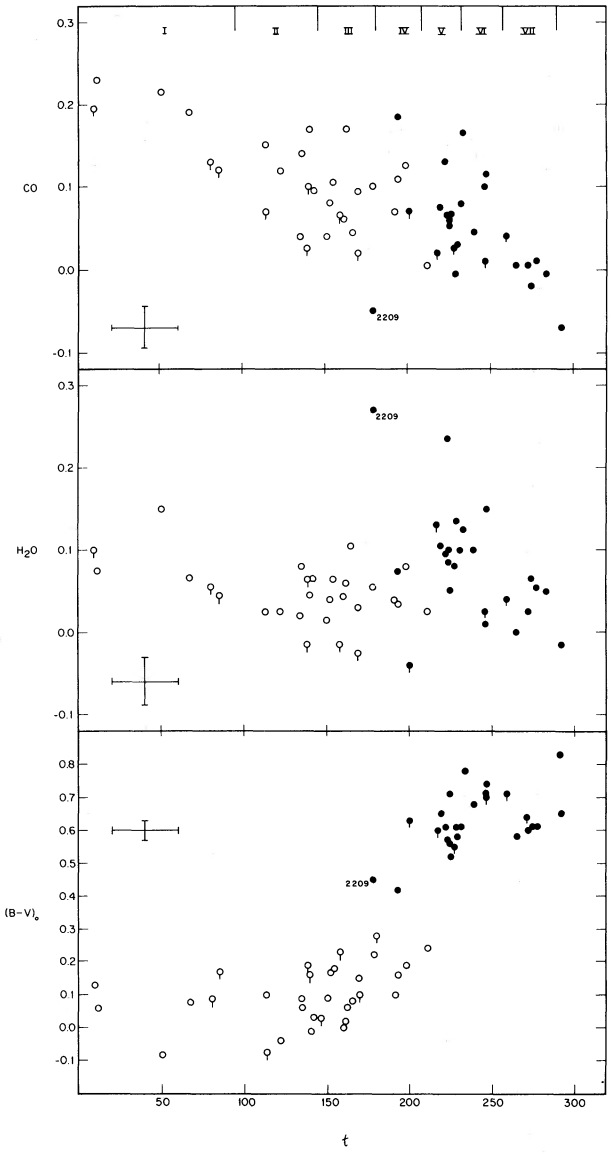

FIG. 3.—Same as Fig. 2, for $B-V$ and narrow-band CO and H_2O indices.

found in the figure captions.[6] Figure 5, CO versus $(J-K)_0$, has been plotted twice; clusters that have been assigned to SWB groups are identified in Figure 5*b* as follows: 1 stands for I, 2 for II or III, 5 for IV, V, and VI, and 7 for VII.

In the last section it was shown that clusters with relatively red infrared colors are confined to a specific range of age. It will be useful to establish criteria, based only on infrared colors and indices, to distinguish these objects—henceforth called "IR enhanced"—from the rest, including other members of the same SWB groups.

[6] Some of the clusters plotted in the two-color diagrams do not appear in the color versus t plots of Figure 2 because their *uvgr* colors have not been measured. This incomplete overlap does not affect any of our conclusions.

We adopt the requirements $(J-H)_0 > 0.6$ and $(H-K)_0 > 0.2$ to define the IR enhanced clusters. This group, located above and to the right of the dividing line in Figure 4, is essentially identical to the group having $(J-K)_0 > 0.8$ and CO < 0.2 in Figure 5 and to that with $(V-K)_0 > 2.5$ and CO < 0.2 in Figure 6. The IR enhanced clusters so defined are noted in Tables 4 and 5.

Group VII clusters resemble old, metal-poor galactic globular clusters (SWB; Gascoigne 1966; Tifft 1963; Hesser, Hartwick, and Ugarte 1976), and the infrared data support this result. The $J-K$ and $H-K$ colors are blue, near 0.6 and 0.1, respectively, and the $V-K$ colors are near 2.0. In Figure 5*b* they are seen to lie at the blue end of the distribution of M31 and Milky Way globulars. There is some scatter among the group VII objects, and several of them have weaker CO absorption than their counterparts in our Galaxy. To within the observational uncertainties however, we cannot say whether or not the bluest objects are actually more metal poor than the most metal-poor systems in the Galaxy.[7]

[7] One interesting object found among the "old" clusters is Hodge 11. Gascoigne (1966) singled it out as a member of a small group of objects having no galactic counterpart, and Walker (1979*a*) estimated its age to be 0.6×10^9 years. Freeman and Gascoigne (1977) and SWB, on the other hand, argue that it is an old metal-poor cluster. The integrated light data presented here show that Hodge 11 is similar to the Milky Way and M31 globular clusters. Also, the two reddest stars in the cluster were observed in the infrared by Aaronson and Mould (1982); they fall at the tip of the M92 giant branch. These results are consistent with Hodge 11 being metal poor (which is not in dispute) and *also old.*

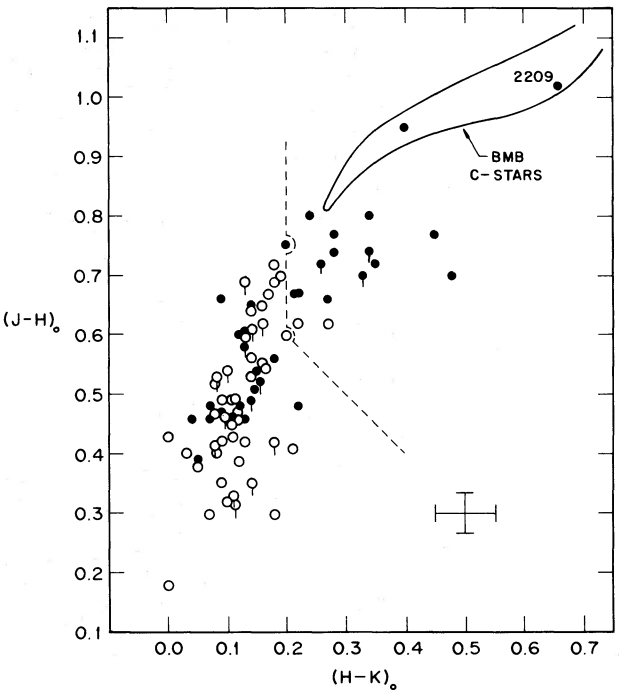

FIG. 4.—The reddening-corrected $(J-H)_0$ and $(H-K)_0$ colors are plotted from the data in Tables 4 and 5. The carbon star region is drawn using the data in CFPE (see subsequent figures). Open and closed symbols are as in Fig. 2.

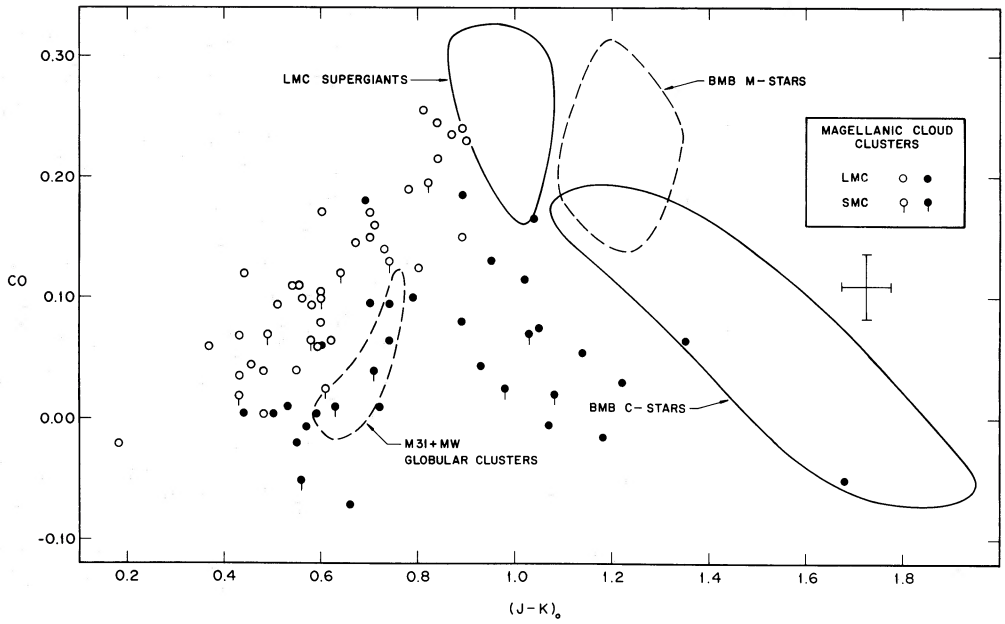

FIG. 5*a*

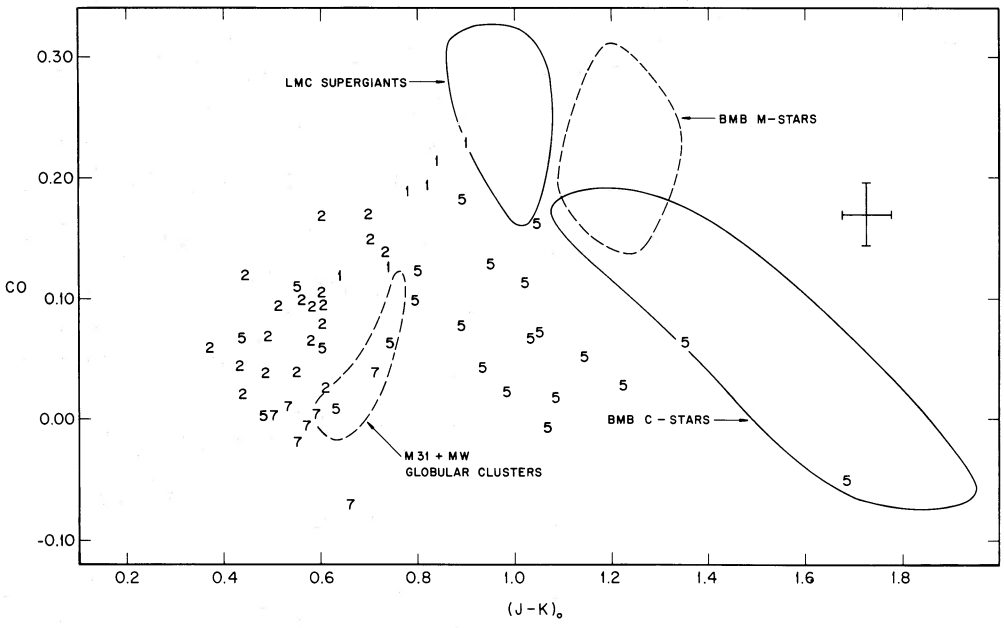

FIG. 5*b*

FIG. 5.—The reddening-corrected CO index is plotted against $(J-K)_0$ for SMC and LMC clusters (data from Tables 4 and 5). The regions enclose most of the individual star and cluster data from the following sources: BMB C and M stars: CFPE; M31 and Milky Way globular clusters: Frogel, Persson, and Cohen (1980*b*) and Aaronson *et al.* (1978); LMC supergiants: Elias *et al.* (1981) and Elias, Frogel, and Humphreys (1983). Open and closed symbols are as in Fig. 2. Fig. 5*b* repeats 5*a* but with numbers referring to cluster data points in the following SWB groups: 1 = I; 2 = II and III, 5 = IV, V, and VI; 7 = VII.

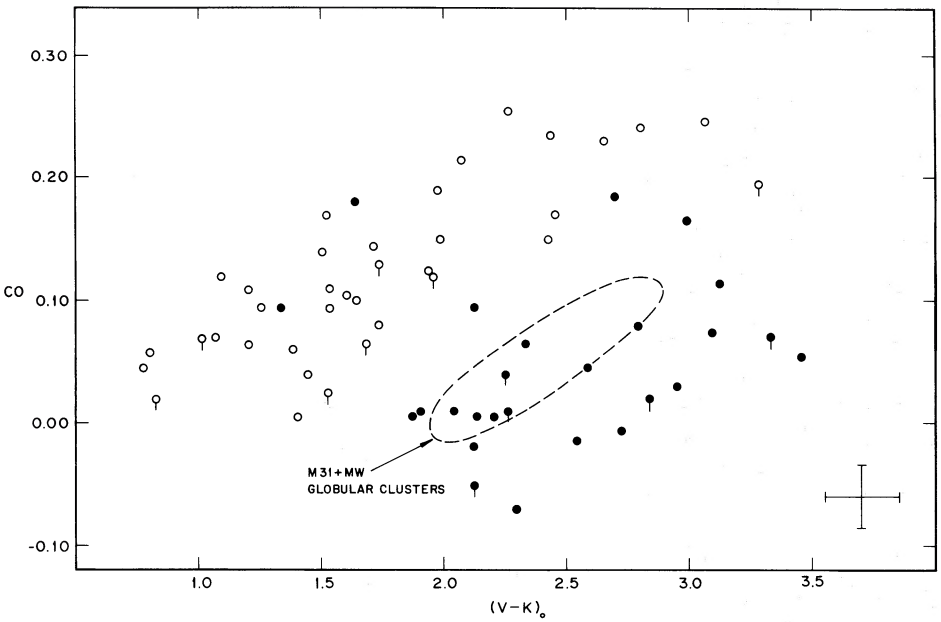

FIG. 6.—Same as Fig. 5*a*, but for the $(V-K)_0$ color

The clusters in groups IV–VI which belong to the IR enhanced group have colors that are very different from those in group VII. For individual giants in the field and in Galactic globular clusters, and for the integrated light of globular clusters the CO index normally increases with infrared color. However, Figure 5*b* shows that for these clusters the CO index tends to *decrease* with increasing $(J-K)_0$ color. Such a trend, which associates red *JHK* colors with weak CO, indices is exhibited strongly by carbon stars (Frogel and Hyland 1972; Frogel, Persson, and Cohen 1980*a*; CFPE). Late-type dwarfs also display red $H-K$ colors, strong H_2O indices, and weak CO (Persson, Aaronson, and Frogel 1977), but their $J-H$ and $J-K$ colors never exceed 0.62 and 0.96 mag, respectively, whereas essentially all of the IR enhanced clusters have $J-H > 0.6$. Therefore, while late-type dwarfs could contribute some fraction of the near-infrared light for the bluer intermediate-age clusters, they cannot account for the observed trends in colors and indices for the IR enhanced clusters. Spectroscopic studies of individual red stars in a number of Cloud clusters show that many members of groups IV, V, and VI do contain carbon stars (Feast and Lloyd Evans 1973; Mould and Aaronson 1979, 1980; Blanco and Richer 1979; Aaronson and Mould 1982; Lloyd Evans 1980; Frogel and Cohen 1982; Frogel and Blanco 1982). With the exceptions of NGC 1994 and 2100, every cluster in the IR enhanced group is known to contain at least one luminous, red carbon star similar to those in LMC fields and studied by CFPE. Three clusters of types IV–VI, NGC 416, 1783, and 1831 and two unclassified clusters, NGC 1916 and K3, also contain luminous, red carbon stars, but are not members of the IR enhanced group. Faint blue C stars have been found in few type VII clusters by the above authors, but it can be easily shown that these stars do not make a significant contribution to the integrated colors or luminosities of the type VII clusters. Frogel, Persson, and Cohen (1980*a*), CFPE, and Frogel and Cohen (1982) have shown that the infrared colors of individual carbon stars in clusters and in the general fields of the Clouds are indistinguishable in the mean.[8] Thus the relative

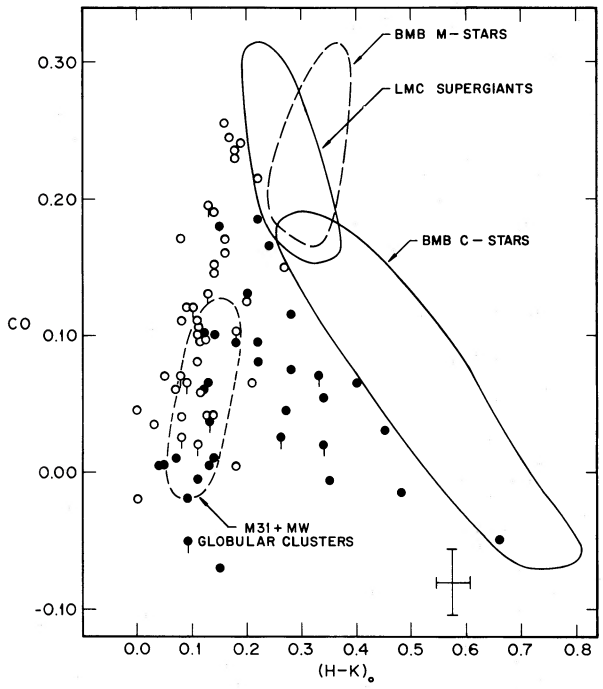

FIG. 7.—Same as Fig. 5*a*, but for the $(H-K)_0$ color

[8] Small differences between the colors of SMC and LMC carbon stars do exist, but are not important in this context.

locations of the field carbon stars and the IR enhanced clusters in Figures 5 and 7 strongly supports the idea that *carbon stars are needed to explain the integrated cluster infrared colors.* The important constraint is the CO index. The low CO indices of the clusters cannot be manufactured by a superposition of warm M stars having weak CO bands—these stars do not have very red broad-band colors. More quantitative support for this conclusion will be presented in § IV.

We now consider the "open" clusters, many of which Hodge (1961) classified as young, populous clusters. All but one of these 31 clusters belong to SWB groups I–IV and have $t < 200$. (NGC 1831 is in group V and has $t = 211$.) These clusters show a well defined dependence of CO strength on $J-K$ and $H-K$ color (Figs. 5 and 7). The CO index behaves similarly as a function of $V-K$, but with more scatter (Fig. 6).

The open clusters are well separated from the M31 and Milky Way globular clusters, as well as from the SWB type VII clusters, in that the former have significantly stronger CO indices at a given $J-K$ and $V-K$ color than the latter groups. They are easily distinguishable from the IR enhanced clusters as well. Of the 31 open clusters, only NGC 2100 and NGC 1993 have $J-H > 0.6$ and $H-K > 0.2$. The open clusters are generally confined to the region $J-K \leq 0.8$, $H-K \leq 0.2$, $V-K \leq 2.0$, or CO ≤ 0.20, and thus are, with few exceptions, separated from the IR enhanced clusters in Figures 5, 6, and 7.

Among the open clusters which have been searched for carbon stars, only NGC 1831, already singled out above, gave a positive result (Aaronson and Mould 1982). In particular, of the SWB types III–IV and IV in which carbon stars have been sought, only in those classified as globular by van den Bergh and Hagen (1968) have carbon stars been found. It is clear from published CMDs that progressively younger clusters contain proportionately more bright red supergiants (see the compilation by Alcaino 1975 and more recent work by Flower and Hodge 1975); their stellar populations can be characterized as combinations of basically two groups of stars, one with $B-V \leq 0.0$, and one with $B-V \geq 1.6$. The correlation of strong CO with red broad-band infrared colors is consistent with an increasing contribution from M giants or supergiants to an underlying blue stellar population. The presence of the blue population can be seen in the $B-V$ versus t plot of Figure 3. For the very youngest objects (with small values of t) the CO indices are as large as are seen in individual late-type supergiants.

c) *Summary of First Order Observational Results*

Plots of color versus age parameter t together with two-color diagrams in which the Cloud clusters are compared to late-type stars lead to the following results:

1. The oldest clusters in the Magellanic Clouds have similar infrared properties to their analogs in the Milky Way and M31.

2. Clusters which are members of an IR enhanced group defined by their JHK colors are almost all of intermediate age, i.e., in SWB groups IV–VI. Nearly all of them also contain red, luminous carbon stars which are needed to account for the infrared colors and indices.

3. At an age near 1×10^9 years a substantial shift occurs in the broad-band colors $J-K$, $H-K$, $V-K$, and $B-V$. The carbon stars in the SWB groups IV, V, and VI have apparently disappeared from the younger groups, to be replaced by M stars which have strong CO absorption and $J-K$ colors that are considerably bluer than those of carbon stars.

4. Clusters which have been classified as "open" can, with few exceptions, be easily distinguished from old, true globular clusters and from intermediate age clusters via infrared photometry alone.

5. The infrared colors of the youngest clusters appear to require a significant contribution from supergiant M stars. This is qualitatively consistent with available CMDs for these objects.

IV. ANALYSIS OF THE INTEGRATED INFRARED LIGHT OF THE INTERMEDIATE-AGE CLUSTERS

a) *Motivation*

From a purely qualitative look at the integrated infrared colors it has been possible to isolate a group of "IR enhanced" clusters which are clearly separated from other clusters, including ones in the same SWB groups, by their infrared colors alone. Almost all of these clusters are known to contain red, luminous carbon stars. In order to proceed with a quantitative analysis of the integrated light of these and other intermediate age clusters we will make the reasonable and simplifying assumption that the light from the underlying stellar population in these clusters, i.e., the light from the main sequence stars, horizontal branch stars, subgiants, and first ascent giants, can be approximated by light from clusters in the region labeled M31+MW clusters in Figures 5, 6, and 7. The main question to be addressed then is: What fraction of the light at K, or bolometrically, is contributed by carbon stars as a function of age? This question is important to the theory of stellar evolution on the asymptotic giant branch (AGB) and to the nature of the overall stellar population, but it is also relevant in a different context. AGB carbon stars have now turned up in the Local Group Carina dwarf galaxy (Cannon *et al.* 1981) and in the Fornax dE galaxy (Demers and Kunkel 1980; Demers Kunkel, and Hardy 1979; Aaronson and Mould 1980; Frogel *et al.* 1982) in addition to the SMC and LMC, and are also known to be common in the galactic anticenter. Their importance in the integrated infrared light of some of the Cloud clusters suggests that they may be detectable in the integrated light of galaxies or parts of galaxies that fall in the appropriate range of age and/or metal abundance. In principle, then, one could obtain age estimates (or constraints) for external stellar populations *if* the infrared measurement precision were sufficiently high (see § IV*d* below).

We shall first analyze the cluster light to show how important the AGB is to the overall energy output of

intermediate age clusters. Next, we substantiate the validity of our analysis of the integrated light by comparing our results with those of recent surveys for carbon stars in Cloud clusters.

b) Analysis

The infrared colors are conveniently analyzed in a flux ratio diagram, as introduced by Rabin (1982). Rather than plot colors, one plots ratios of fluxes, from which the component fractions of the composite light can be read off in a straightforward way. Figure 8 is the flux ratio analog of the $CO/(H-K)$ plot of Figure 7.[9]

The four regions marked on Figure 8*a*, analogous to the regions in Figure 7, enclose most of the stars and clusters we believe represent the likely consituents of the Cloud cluster light. (The sources for the data used to draw the regions are given in the legend to Fig. 4.) The particular supergiants observed and used to draw the supergiant region were selected from those with the highest luminosities. Their colors and CO indices are similar to those of the M stars from the BMB survey, so we expect that any supergiant of intermediate luminosity will also display a similar color and CO index.

Analysis is restricted to the $CO/(H-K)$ diagram, because these wavelengths are most strongly confined to the infrared and hence less subject to dilution by bluer stars on the main sequence and subgiant branch. In fact, the $H-K$ colors of the younger (*open circle*) clusters are similar to those of the M31 and Milky Way globular clusters in Figures 7 and 8.

Figure 8*b* is a schematic plot of Figure 8*a*. As shown by Rabin (1982), the combination of any two components (points) in such a diagram is located at some point on the straight line connecting them. The *relative* contribution of the two components to the light in the composite system at the wavelength which is the common denominator of both axes is proportional to the distances to the point representing the composite system from the two components. For example, let us start with the colors of a metal-poor globular at point *b*. If we add to this cluster carbon stars with colors characteristic of point *f*, the colors of the resulting system must lie on the line segment *bf*. At point *c* on this segment carbon stars are contributing a fraction *bc*/*bf* of the total observed flux at *K*. One can go on in this manner by adding light from a metal-rich globular, for example, at point *a* to the system at point *c*. The three component system would then lie on segment *ac*.

[9] $H-K$ color has been replaced by the parameter H/K, the ratio of fluxes at 1.65 and 2.2 μm. The CO index has been replaced by the ratio of fluxes at 2.36 and 2.20 μm (see Frogel *et al.* 1978). We have labeled this parameter $2.36/K$ and have ignored any small color terms relating the 2.20 μm and K magnitudes.

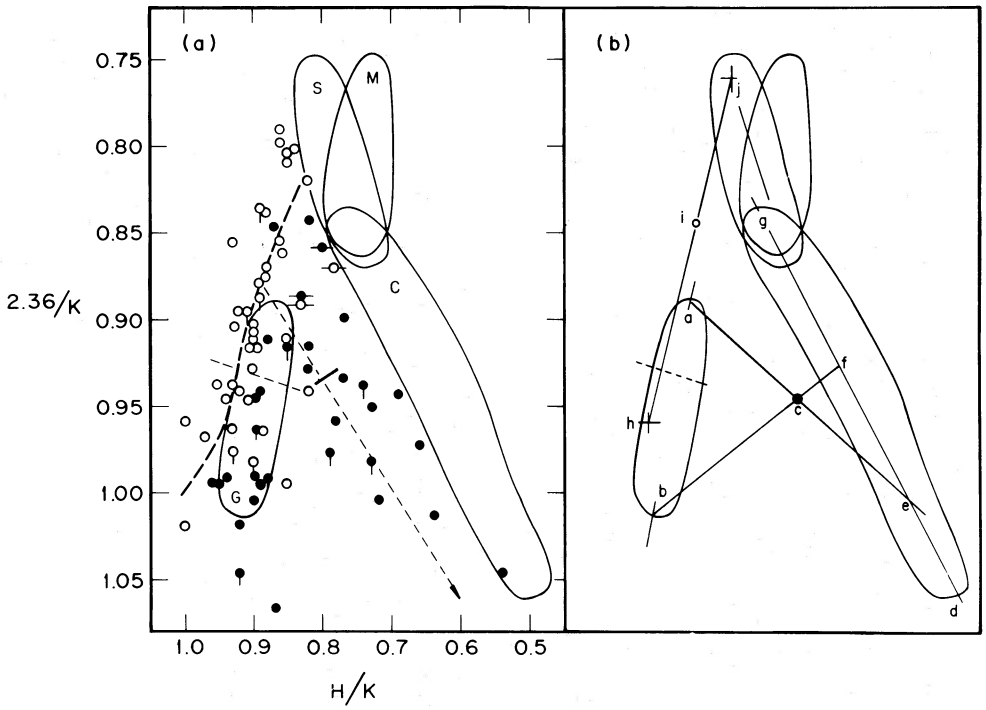

FIG. 8.—(*a*) Flux ratio diagram (following Rabin 1980, 1981) corresponding to the CO vs. $H-K$ diagram of Fig. 5. The supergiant, M star, BMB carbon star, and M31 plus Milky Way cluster regions of Fig. 5 are indicated here by the letters S, M, C, and G, respectively. The heavy dashed line running up and to the right is the locus for individual metal-rich giant stars. The thin dashed line which cuts through region C divides the younger clusters (*open circles*) into two groups, analyzed in § V*a* for supergiant contribution. The dashed line running down and to the right is the locus of composite cluster light having $(2.36/K, H/K) = (0.88, 0.89)$, mixed in varying proportions with carbon star light, as discussed in § V*b*. The four points flagged with horizontal lines are NGC 1994, 2107, 2162, and 2173. (*b*) Repeats the regions of Fig. 8*a* together with a number of fiducial locations used to analyze the carbon star and supergiant contributions to the integrated light. See §§ IV*b* and V*a*.

The ridge line of the carbon star distribution line *dg* is taken to represent the carbon star population, since the width of the region is close to the observational uncertainties. Points *a* and *b* are taken to represent the extremes of the underlying cluster colors. There are 20 clusters within the region *abdg*, most of which are members of the IR enhanced group. We assume for the moment that the clusters lying within the M31 plus Milky Way region—labeled G in Figure 8*a*—contain no carbon stars, but later on we will return to specific cases in which this assumption is incorrect. If point *b* represents the light from an underlying cluster (the same for each of the 20 observed clusters), then the average fraction of the *K* light contributed by C stars, assuming they all lie in region C (i.e., the average value of *bc/bf*), is 0.64 with a 1 sigma dispersion of 0.16. Alternatively, if point *a* is taken to represent the underlying cluster, the mean carbon star fraction is found to be 0.40 ± 0.18. For clusters lying much below point *c*, the extension of segment *ac* does not intersect the carbon star domain (segment *gd*), so the underlying cluster must lie closer to point *b*. In Figure 8*a*, four clusters, NGC 1994, 2107, 2162, and 2173, are flagged with horizontal bars. NGC 1994 and 2173 belong to the IR enhanced group. They lie in a region intermediate between the open clusters having strong CO absorption and the globulars with weak CO and red $H-K$ colors. These clusters thus may not contain carbon stars, but rather could contain bright M stars; the present data do not distinguish between these possibilities.

The 2.2 μm luminosity due to carbon stars alone for each of the 20 clusters analyzed was computed from the data in Tables 2 and 3, and compared with the median apparent 2.2 μm magnitude for the BMB sample of field carbon stars (CFPE), which is the same as that found for cluster carbon stars (Frogel and Cohen 1982). The median magnitude for these stars is $K = 10.3$ with quartiles at 10.6 and 9.9. For each cluster the 2.2 μm magnitude in the largest aperture was used. Adopting 10.3 as the fiducial single carbon star *K* magnitude leads to an average of 2.5 carbon stars per cluster. This number is small enough that stochastic effects must be important; it is plausible, in fact, that all the scatter in the cluster $J-K$ and $H-K$ colors arises solely from this effect.[10]

The 0.6 fraction of the *K* light due to carbon stars can be converted to a corresponding fraction of the bolometric luminosity by using the dependence of the bolometric correction BC_K upon $J-K$ color as given by Frogel, Persson, and Cohen (1980*a*). The fraction of the bolometric luminosity due to carbon stars is, in general, less than that at *K* because the *K* band is closer to the peak of the energy distribution of the warmer underlying cluster. Simple models were constructed to show that a fraction 0.6 at *K* corresponds approximately to 0.5 bolometrically. The median bolometric magnitude of the carbon stars used in the analysis is -4.8, which is 1–1.5 mag brighter than the tip of the first ascent giant branch. Thus on average, half of the energy output of the clusters in the "intermediate-age" domain is due to the consumption of fuel in carbon stars on the asymptotic giant branch *above* the tip of the first red giant branch. According to the age calibration of the SWB classification offered by Aaronson and Mould (1982), the age range over which this proportion could be important to the bolometric energy output of a system of stars could extend from ~ 1 to 6×10^9 years. This fractional contribution of AGB stars to the bolometric luminosity of a system really is only a lower limit since many of the clusters have luminous AGB M stars as well, although they generally are fainter than the C stars (Frogel and Cohen 1982).

c) *Comparison of the Clusters' Carbon Star Content Derived from Their Integrated Light with That from Recent Surveys*

A rather large number of Cloud clusters have now been surveyed for carbon stars. They have been identified spectroscopically or through their near-infrared colors, following photographic selection by extremely red color. The work of Feast and Lloyd Evans (1973), Mould and Aaronson (1979), and Frogel, Persson, and Cohen (1980*a*) has been extended through the surveys of Mould and Aaronson (1980), Aaronson and Mould (1981), Frogel and Cohen (1982), Blanco and Richer (1980), and Lloyd Evans (1980).

All available infrared photometry for carbon stars in the present sample of SWB type IV, V, and VI clusters was compiled from the sources listed above. The finding charts given by Aaronson and Mould, Lloyd Evans, or in earlier work were used to locate the stars and then to compare the carbon star contributions at *J*, *H*, and *K*, to the multiaperture data for each surveyed cluster.

The (known) carbon star contributions were subtracted from the relevant multiaperture data points to look first at the colors and color gradients remaining in the underlying cluster light. The fractional contribution to the light at 2.2 μm due to known carbon stars was also found for the largest aperture data point for each cluster. The results are given in Table 6, which lists in successive columns the aperture diameter within which survey stars were found, the fractional contribution at 2.2 μm due to these carbon stars, and the analogous quantity derived in § IV*b* above from integrated light data. The $H-K$ colors listed are the approximate colors of the underlying cluster after removal of the survey carbon stars present. The notes

[10] NGC 2231 is too faint to contain even one carbon star at $K = 10.3$, and thus it must contain red carbon stars that are fainter than the mean. NGC 1994 is bright, and by the simple analysis could contain ~ 16 carbon stars at $K = 10.3$, whose summed light would have to lie near point *g* in Figure 8*b*. This is quite unlikely however, because carbon stars in both the field and cluster samples are fairly uniformly spread out in $H-K$ color; point *f* is a more likely location for the superposition of 16 LMC or SMC carbon stars. Aaronson and Mould (1982) found three bright red stars in NGC 1994; their $J-K$ colors are not as red as those of carbon stars. On both counts, therefore, the integrated light of NGC 1994, is probably due mostly to bright M stars. This is not surprising since NGC 1994 lies near the strong CO boundary of the IR enhanced group in Figures 4–7, and is also classified as an open cluster.

TABLE 6

FRACTIONAL CARBON STAR CONTRIBUTIONS AT 2.2 MICRONS

CLUSTER (1)	APERTURE DIAMETER (arcsec) (2)	NO. OF C STARS FROM SURVEYS (3)	CARBON STAR FRACTION AT 2.2 μm: From Surveys (4)	CARBON STAR FRACTION AT 2.2 μm: From Analysis of Integrated Light (5)	$(H-K)$ OF RESIDUAL CLUSTER (6)	NOTES (7)
NGC 152	60	2	0.36	0.56	0.33	1
NGC 416	60	0	0.0	0.0	0.14	
NGC 419	60	8	0.40	0.50	0.20	5
K3	60	1	0.13	0.0	0.08	2
NGC 1751	60	2	0.36	0.54	0.18	3
NGC 1783	60	2	0.18	0.0	0.08	1
NGC 1806	60	2	0.28	0.35	0.15	2
NGC 1831	59	1	0.39	0.19	0.13	2,6
NGC 1846	60	2	0.23	0.46	0.24	2
NGC 1916	56	1	0.08	0.0	0.14	1
NGC 1978	60	1	0.16	0.41	0.18	1
NGC 1987	60	2	0.33	...	0.25	2, 5, 6
NGC 2107	60	0	0.0	0.36	0.21	6
NGC 2108	64	1	(0.22)	0.68	0.43	4
NGC 2121	60	0	0.0	0.64	0.40	
NGC 2154	64	2	0.57	0.71	0.24	2
NGC 2155	30	0	0.0	0.0	0.16	
NGC 2162	30	0	0.0	0.36	0.21	6
NGC 2173	30	0	0.0	0.69	0.25	6
NGC 2209	30	2	(large)	0.87	...	5
NGC 2213	64	2	0.66	0.50	0.01	2

[1] The survey carbon star(s) do not completely account for the color changes with aperture. See text.
[2] The presence of carbon stars most likely produces the observed color gradients seen in Tables 2 and 3.
[3] The presence of carbon stars in both small and large apertures is consistent with the lack of color gradient.
[4] Infrared photometry of Lloyd Evans star no. 1 in NGC 2108 is not available. Note 2 could apply, depending on its colors and magnitude.
[5] NGC 419, NGC 1987, and NGC 2209: see text.
[6] Special cases plotted in parentheses in Fig. 9, because integrated light colors do not demand the presence of carbon stars; see text.

following Table 6 describe the results of the color gradient test.

In assessing the validity of the results, three caveats should be borne in mind. First, the centering errors (noted in Tables 2 and 3) can be important for clusters containing only a few bright carbon stars; second, the carbon stars may be slightly variable; and third, the different carbon star surveys are not homogeneous, nor are they all complete in the central regions of concentrated clusters. For these reasons we have not attempted to assign uncertainties to the numerical values derived.

The survey and integrated light fractional carbon star contributions are plotted in Figure 9. Figure 9 shows that although there is nonnegligible scatter, integrated light photometry is quite useful in establishing the presence of carbon stars in stellar systems. It also appears that the carbon star fraction deduced from integrated light photometry is somewhat higher than that deduced from surveys; note the shift of the data points away from the 45° line in Figure 9. The average difference between columns (4) and (5) of Table 6 is 0.12 ± 0.06, a 2 σ_m result for 16 clusters. The $H-K$ colors of the residual (underlying) clusters, as found by removing known carbon stars from the infrared photometric data

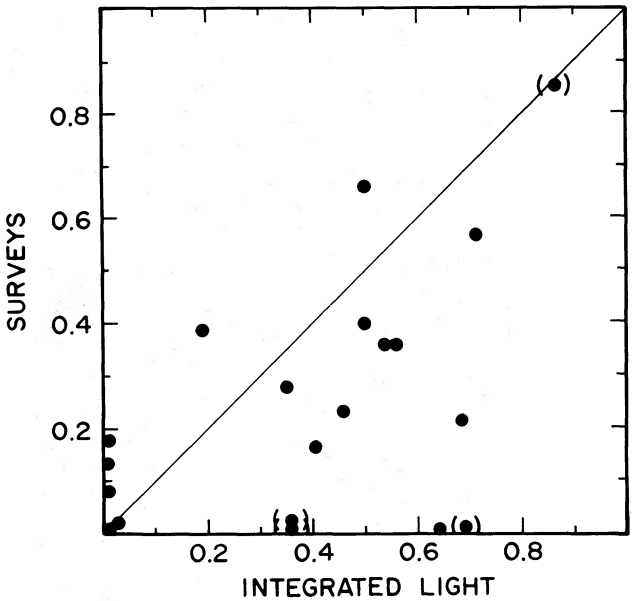

FIG. 9.—Comparison of the fractional contribution to the 2.2 μm light of carbon stars of intermediate-age clusters from survey results and from integrated light analysis. See § IV*c*.

points, are listed in column (6) of Table 6. The average residual $H-K$ color for 16 clusters is 0.19 ± 0.03 ($1\ \sigma_m$) mag; the median residual $H-K$ color is 0.18. This color is $2\ \sigma_m$ *redder* than the color of $H-K \sim 0.12$ which is the average color for the Milky Way and M31 globular clusters in Figure 5. This result seems to indicate that the carbon star surveys are not giving us the complete picture of the clusters' carbon star content. Because of the three caveats noted above, the result is not unequivocal; nevertheless, it seems possible that there are additional (faint?) carbon stars in the clusters. Four clusters, NGC 2107, 2121, 2162, and 2173, appear from the integrated light results to contain carbon stars, but not from the survey results. We recall that NGC 2107, 2162, and 2173 were considered special cases in the integrated light analysis, because their CO indices are so large that it was not at all obvious that they should be included in the carbon star clusters (cf. IV*b*). These three clusters plus NGC 1987 have been plotted in parentheses (see Table 6).

The notes to Table 6 give the results of the color gradient tests. The color gradients seen in the multi-aperture data of Table 2 are, in seven cases, completely explained by the presence of carbon stars found in surveys. In two cases the lack of a color gradient is consistent with the survey results, and in four cases the survey stars do not completely account for the observed color gradients.

The results in Table 6 for NGC 419 and NGC 2209 require comment. NGC 419 is clearly rich in luminous carbon stars, and the integrated light analysis results agree well with the survey. With eight carbon stars detected in a 60″ beam, the stochastic effects are reduced, and the infrared colors of NGC 419 should represent more realistic colors of a stellar population of this particular age and metal abundance. Its intermediate location in the color versus t plot (Fig. 2) bears this out. There is weak evidence for additional carbon stars in the bright central regions, as the fraction of the light at 2.2 μm due to (survey) carbon stars drops from 0.4 in a 60″ beam to 0.2 in a 30″ beam. On the whole, however, NGC 419 demonstrates that the analysis procedures work well.

NGC 2209 represents the opposite extreme, where the two carbon stars W46 and W50 dominate the energy output. Star W50 at $K = 10.03$ (Aaronson and Mould 1982; Frogel and Cohen 1982) accounts for nearly half the light in a 30″ beam. It seems likely, therefore, that the infrared centering was affected by either W46 or W50; although W46 is closer to the visual center of the cluster, it is not as red as the "cluster" as measured with a 30″ beam. Despite these systematic uncertainties in the measurements of NGC 2209, the main point is not lost, viz., the energy output is truly dominated by two stars whether or not the centering was affected.

d) Detectability of Intermediate-Age, Metal-Poor Populations

The infrared colors of a pure group V intermediate-age, metal-poor (SMC) population should be similar to those of NGC 419. This cluster, as noted above, is bright enough and contains sufficiently many carbon stars that the stochastic effects upon the infrared colors are minimized. The differences in colors between such a population and a similarly metal-poor but old (group VII) population are $\Delta J-K \sim 0.4$, $\Delta H-K \sim 0.18$, and $\Delta K \sim \Delta V-K \sim 0.8$, in the sense that the carbon-star dominated population will be redder and brighter in the infrared. It seems possible that evidence for such a population type could be detected in globular clusters of external galaxies, in young metal-poor dwarf galaxies, or perhaps in the external regions of spiral galaxies. The measurement precision required to detect as little as a 30% contribution from such a population would, however, be high.

e) Comparison of the SMC versus the LMC Clusters in Integrated Light

Figure 2 shows that there are no obvious differences in any of the colors or indices between the clusters of the SMC and LMC, with the possible exception of the CO indices being $\sim$0.04 mag stronger on average in the LMC open clusters than in those of the SMC. This one exception is consistent with the results of McGregor and Hyland (1982), who showed that individual red supergiants in the two systems differ systematically in their CO indices—a dependence which they have explained in terms of the higher heavy-metal abundance of the LMC.

Even though only four carbon-star dominated clusters (in groups IV, V, and VI) in the SMC have been measured, the approximate equality of the integrated light of these cluster colors and ones of corresponding type in the LMC indicates roughly equal proportions of carbon stars in the two cluster systems, a situation quite different from that found by BMB for the C/M star ratio in fields of the two Clouds. The C/M star ratio varies from $\sim$2 in the LMC to $\sim$20 in the SMC, a difference which we might have expected to show up in the broad-band infrared cluster colors. These apparently contradictory results are understandable when proper account is taken of the BMB survey techniques and differences between the field and cluster M stars (Frogel and Cohen 1982). First, the BMB survey selects only those M stars later than M5. Because the SMC has a lower metal abundance, it is expected to have a smaller proportion of such stars than the LMC (see Frogel *et al.* 1982). This effect alone accounts for most of the apparent discrepancy. Second, Frogel and Cohen (1982) have shown that the cluster M stars in both systems are significantly fainter and bluer than the LMC field M stars, and are almost always fainter than the faintest cluster C star. Thus the domination of the integrated infrared cluster light by carbon stars tends to mask any differences between the two cluster systems brought about by differences in their content of bright (AGB) M stars.

V. THE YOUNG CLUSTERS

a) Clusters in Groups I–III

We now turn to the younger clusters. Available CMDs and theory for clusters in this age range indicate that there will be a large contribution from early main

sequence and main sequence turnoff stars to the light at any wavelength; the blue integrated $B-V$ colors for these groups compared to the older groups attest to this fact. The CMDs and spectroscopic surveys also show the presence of luminous M supergiants, particularly in the youngest clusters; these stars should be important at longer wavelengths. If we restrict attention to the $H-K$ color in order to analyze the infrared light, the blue light contribution should be much reduced. Figures 7 and 8 show a rather good correlation between CO and $H-K$ in groups I, II, and III. The heavy dashed line on the left side of Figure 8*a* shows the run of CO with $H-K$ for individual giant stars. This steady increase of CO with $H-K$ suggests that these open clusters are composed of light having the colors of point *h*, for example, plus a steadily increasing contribution from luminous red stars with strong CO. If this is the case, then these clusters cannot contain carbon stars in the same proportion as do the IR enhanced clusters in groups IV–VI. Point *i* represents a sample superposition with a 58% contribution at 2.2 μm from supergiant stars at point *j*. We have taken the median flux ratio values for the clusters below the dashed line in Figure 8*b* to get the colors of point *h*, and have used supergiant colors for an illustrative computation. There are then 30 clusters near *hij*, including the three which could contain carbon stars (2107, 2162, and 2173). The average fractional contribution at 2.2 μm due to red supergiants in those 10 clusters which have been classified into groups II and III is 0.33. For those classified in group I (six clusters) it is 0.55. The remaining clusters are the transition cases noted plus NGC 2134 and NGC 1987.[11]

In Figure 3 and Table 4 and 5 the six clusters with values of $t < 100$ (SWB type I) are seen to display uniformly large CO indices and a range in all the broad-band infrared colors. The reddest object is the SMC cluster NGC 299 with $(V-K)_0 = 3.39$, and the bluest is NGC 300 with $(V-K)_0 = 1.84$. There are not enough very young clusters to be sure that the apparent systematic decrease in CO with increasing t is real. Figure 4 shows that the CO indices and broad-band colors of the youngest clusters lie near those of a sample of red supergiants in the field of the LMC. Qualitatively, then, a likely picture for the composition of the infrared light is that the 2 μm region is dominated by a few red supergiants. As the blue region of the spectrum is dominated by the light of bright blue stars, the integrated color of the system depends sensitively upon the exact numbers of the brightest blue and red stars; this accounts for the wide range in integrated light $V-K$ colors. Figure 8 suggests that ~80% of the 2.2 μm light and hence at least half of the bolometric luminosity is due to red supergiants.

The average contribution at 2.2 μm from red supergiants for all 30 clusters is 0.51 ± 0.21 (1 σ dispersion) and thus for the younger clusters the contribution from luminous red stars, is substantial. (The four ambiguous clusters [Fig. 8*a*, flagged points] were assumed to be comprised of supergiants lying in the intersection of the supergiant and carbon-star regions.) Thus, although the younger clusters do appear to be strongly affected by AGB stars, as were the clusters in groups IV–VI, the most luminous stars in the young clusters do not appear to be carbon stars. NGC 2209 at $t = 178$ (age $\sim 10^9$ years; Gascoigne *et al.* 1976) is the earliest SWB type cluster known which does contain luminous carbon stars, and in any case it is classified as a group III–IV. Note that we make no statement about the absolute numbers of carbon stars detected (groups IV, V, and VI) or not detected (groups II, III). We *are*, however, comparing roughly equal bolometric luminosities of the underlying clusters which either contain or do not contain carbon stars.

b) The Lack of Carbon Stars in Groups II and III

The apparent lack of bright carbon stars in groups II and III is analogous to the situation for field carbon stars (see CFPE). A t of 180, below which the integrated colors imply few luminous C stars, corresponds roughly to an age of 1×10^9 years and a turnoff mass of $\sim 2\ M_\odot$. This mass is so far below the upper limit of $8\ M_\odot$ for the main sequence stars believed to be the precursors of carbon stars (see, e.g., Iben and Truran 1978) that we might expect to see a few carbon star members in these objects. As discussed by CFPE and Richer (1981), the luminosity function for field carbon stars is much fainter overall than that predicted from current theory. Both the Iben (1981) and especially the Renzini and Voli (1981) luminosity functions contain substantial fractions of stars brighter than the brightest carbon star seen in the BMB survey at $M_{bol} = -6.0$. One of Iben's (1981) suggested solutions to this problem is that the missing carbon stars are lurking inside dense dust shells and hence would not be seen in the BMB survey. Such stars, if they exist, could be found in the field, but only in an extensive survey at longer infrared wavelengths. Our new data comprise a survey in the sense that a large-aperture observation of a rich cluster surveys many stars at the same time. If dust-enshrouded stars were actually present in one or more of these clusters, would we have detected them at K? Distances and bolometric luminosities of extremely red carbon stars in the Galaxy are uncertain, but we can nevertheless address the question by investigating the effects they would have on the *colors* of the Cloud clusters. Dyck, Lockwood, and Capps (1974) have presented broad-band observations of four extremely red carbon stars, and we have used Figure 8 to estimate the numbers of such stars which could be present in the group II and II clusters. Table 7 lists the H/K flux ratios and bolometric corrections BC_K of the three red carbon stars for which Dyck *et al.* give total fluxes ($M_{bol} = K + BC_K$). We have also computed the apparent CO indices and $2.36/K$ ratios on the assumption that the 2.29 μm CO band is completely

[11] NGC 1987 is an interesting case: it has strong CO absorption, and is luminous enough to contain many bright stars. Aaronson and Mould (1982) found two probable carbon stars in NGC 1987, which leads us to conclude that NGC 1987 contains bright AGB M stars and carbon stars.

TABLE 7

FLUX RATIOS FOR RED CARBON STARS

Star (1)	$H-K$ (2)	CO (3)	H/K (4)	$2.36/K$ (5)	BC_K (6)
+40485	1.54	−0.28	0.242	1.294	2.85
+50096	1.64	−0.34	0.221	1.368	2.65
+50357	2.10	−0.41	0.145	1.459	2.08

filled in by the circumstellar dust emission and CN absorption (CFPE) in analogy with IRC +10216 (Becklin *et al.* 1969). These flux ratios lie well off the plot in Figure 8*a*; the dashed line running down and to the right is the trajectory for cluster 2.2 μm light composed of an underlying cluster in the main group of points at $H/K = 0.89$, $2.36/K = 0.88$, plus star(s) of the infrared colors of IRC +40485. The tick mark on this trajectory represents the location of a type II or III cluster which displays what we consider to be an easily detectable contribution from such a red star. We note that both H/K and $2.36/K$ are strongly affected by the presence of even one such star: the particular tick mark shown represents a 13.5% contribution from IRC +40485.[12] We now convert this fraction to the bolometric magnitude of a single carbon star detectable against a cluster of observed total magnitude K. The relationships are:

$$M_{\rm bol} = K - 13.6 \text{ for IRC } +40485$$
$$= K - 14.0 \text{ for IRC } +50357 .$$

Among the group II and III clusters observed (including those whose infrared colors alone place them securely in this age group also) only NGC 1850 with $K = 7.74$ in a 60″ diameter aperture is bright enough to conceal a very red carbon star, but even then only if the star has $M_{\rm bol}$ fainter than −6.3. NGC 1850 shows no indication of containing such a star, nor does any other group II or III cluster, 26 in all.

The above exercise cannot test Iben's solution to the bright carbon star problem if the dust shells he proposes are very cool. If the missing stars have energy distributions like that of IRC +10216 (Becklin *et al.* 1969), then they should show up in the survey mode of the *Infrared Astronomical Satellite* (*IRAS*). The sensitivity of *IRAS* at 10 μm (Soifer, private communication) should be such that stars with [10 μm] magnitude <5 will be found at the 10 σ level; this corresponds to $K \sim 12.5$ for IRC +10216. If IRC +10216 is 1 kpc away, the *IRAS* 10 μm limit is 4 mag *fainter* than required to detect an IRC +10216 in the LMC.

c) *Comparison with Published Stellar Synthesis Models*

Struck-Marcell and Tinsley (1978) have presented synthetic models for the integrated infrared and visible colors of systems of stars over a large range in age. Their models were constructed to study the stellar content of young galaxies, but their single burst case should be appropriate for comparison with the light of the Cloud clusters. Although the models are restricted to a single mass function for the main sequence, a single metal abundance (solar), and zero reddening, it is useful to carry out the comparison in order to determine how the models can be improved.

Figure 10 shows the $(U-V, V-K)$-diagram with the Struck-Marcell and Tinsley single burst model superposed. The numbers along the line give the model ages in units of 10^9 years. Their burst lasts for 10^7 years, so it is not to be expected that agreement should be good for the very youngest clusters, with ages less than 0.05×10^9 years. The comparison shows that a serious problem with the theory exists for all of the youngest clusters and many of the intermediate age clusters: the theoretical $V-K$ colors are too blue by up to 2 mag. Reddening the model colors cannot alleviate the problem, as the reddening vector in Figure 10 shows. The answer surely lies in the population of red supergiants which produce the large CO strengths in the youngest clusters. Red supergiants were mentioned as a possible problem by Struck-Marcell and Tinsley, and the new data show that they do indeed produce very strong effects.

Turning to the cluster/model comparison for the older clusters, we see that near 2×10^9 years the observed $V-K$ colors are again considerably redder than the models. This disagreement is due to the presence of carbon stars in intermediate-age, metal-poor objects. These results for the young and intermediate-age clusters indicate that significant revisions to the models are required before they can be used to estimate ages via a comparison of observed and predicted $V-K$ colors.

VI. SUMMARY

The principal observational results are listed in III*c*. From a simple analysis of the infrared colors of the observed clusters in the Magellanic Clouds we conclude the following.

1. Many of the SWB class IV, V, and VI clusters, i.e., the "intermediate-age" objects, contain carbon stars. Most of the clusters with carbon stars can be identified from their integrated infrared colors alone. Thus reliable estimates of the carbon star contributions to integrated light systems in external galaxies can be made. For 20 clusters in which the carbon star contribution is detected in integrated infrared light, on average half the bolometric luminosity is due to them.

2. The findings of conclusion (1) are quantitatively consistent with the results of recent red photographic surveys designed specifically to find cool carbon stars.

3. For the younger clusters in SWB groups II and III, approximately half the light at 2.2 μm comes from luminous oxygen-rich red stars, presumably supergiants. We do not detect carbon-star light in any of the younger clusters. This is consistent with the finding of CFPE that the luminosity function of field carbon stars in the Clouds has an upper bound which is well below the

[12] The open cluster which lies right at the tick mark in Figure 8*a* is NGC 1984, which was not observed by SWB or in the carbon star surveys.

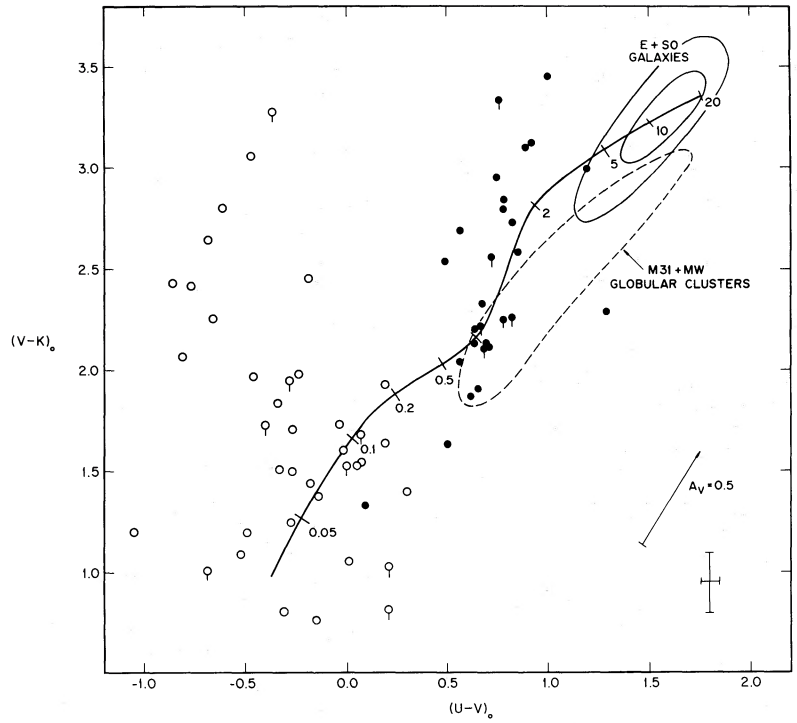

FIG. 10.—Reddening-corrected colors $(V-K)_0$ and $(U-V)_0$ are plotted for LMC and SMC (*flagged points*) clusters. Struck-Marcell and Tinsley's (1978) single burst model is shown as the heavy line; ages in 10^9 years are given along the locus. The regions occupied by M31 and Milky Way globular clusters (Frogel, Persson, and Cohen 1980*b*) and by E and S0 galaxies (Frogel *et al.* 1978) are shown. For the latter, the greatest concentration of galaxy points occurs in the inner region; the outer region encloses nearly all our galaxy data. A reddening vector and representative $\pm 1\ \sigma_m$ error bar are also given.

luminosity at which current theory predicts most of the carbon stars should lie.

4. In integrated infrared light, the only difference between clusters in the LMC and SMC is that the youngest supergiant-dominated objects in the SMC have weaker CO absorption, probably consistent with the established lower metal abundance in the SMC. No difference in the contribution by carbon stars to the total infrared light was found in comparing SMC to LMC clusters.

5. The bulk ($\sim 80\%$) of the 2.2 μm light of the youngest clusters (SWB class I) is from red supergiants. The cluster $V-K$ colors disagree sharply with the colors of evolutionary models which do not include red supergiants.

The work of S.E.P., M.A., and K.M. was supported in part by the National Science Foundation. We are grateful to J. Mould who assisted in making some of the observations at the Las Campanas 40 inch, and to L. Searle for communicating his results to us before publication. We thank an anonymous referee for suggesting a number of improvements.

REFERENCES

Aaronson, M., Cohen, J. G., Mould, J., and Malkan, M. 1978, *Ap. J.*, **223**, 824 (ACMM).
Aaronson, M., Frogel, J. A., and Persson, S. E. 1978, *Ap. J.*, **220**, 442.
Aaronson, M., and Mould, J. 1980, *Ap. J.*, **240**, 804.
———. 1982, *Ap. J. Suppl.*, **48**, 161.
Alcaino, G. 1975, *Astr. Ap. Suppl.*, **21**, 279.
———. 1978, *Astr. Ap. Suppl.*, **34**, 431.
Becklin, E. E., Frogel, J. A., Hyland, A. R., Kristian, J., and Neugebauer, G. 1969, *Ap. J.* (*Letters*), **158**, L133.
Bernard, A. 1975, *Astr. Ap.*, **40**, 199.
Bernard, A., and Bigay, J. H. 1974, *Astr. Ap.*, **33**, 123.
Blanco, B. M., Blanco, V. M., and McCarthy, M. F. 1978, *Nature*, **271**, 638.
Blanco, V. M., McCarthy, M. F., and Blanco, B. M. 1980, *Ap. J.*, **242**, 938 (BMB).
Blanco, V. M., and Richer, H. B. 1979, *Pub. A. S. P.*, **91**, 659.
Cannon, R. D., Niss, B., and Nørgaard-Nielsen, H. U. 1981, *M.N.R.A.S.*, **196**, 1P.
Cohen, J. G., Frogel, J. A., Persson, S. E., and Elias, J. H. 1981, *Ap. J.*, **249**, 481 (CFPE).
Danziger, I. J. 1973, *Ap. J.*, **181**, 641.
Demers, S., and Kunkel, W. E. 1980, *Pub. A. S. P.*, **91**, 761.
Demers, S., Kunkel, W. E., and Hardy, E. 1979, *Ap. J.*, **232**, 84.
Dyck, H. M., Lockwood, G. W., and Capps, R. W. 1974, *Ap. J.*, **189**, 89.
Elias, J. H., Frogel, J. A., Humphreys, R. M., and Persson, S. E. 1981, *Ap. J.* (*Letters*), **249**, L55.
Elias, J. H., Frogel, J. A., and Humphreys, R. M. 1983, in preparation.
Feast, M. W., and Lloyd Evans, T. 1973, *M.N.R.A.S.*, **164**, 15P.
Flower, P. J., and Hodge, P. W. 1975, *Ap. J.*, **196**, 369.
Freeman, K. C., and Gascoigne, S. C. B. 1977, *Proc. Astr. Soc. Australia*, **3**, 136.

Frogel, J. A., and Blanco, V. M. 1982, in preparation.
Frogel, J. A., Blanco, V. M., McCarthy, M. F., and Cohen, J. G. 1982, *Ap. J.*, **252**, 133.
Frogel, J. A., and Cohen, J. G. 1982, *Ap. J.*, **253**, 580.
Frogel, J. A., and Hyland, A. R. 1972, *Proc. 17th International Astrophysics Symposium, Liège*, p. 111.
Frogel, J. A., Persson, S. E., Aaronson, M., and Matthews, K. 1978, *Ap. J.*, **220**, 75.
Frogel, J. A., Persson, S. E., and Cohen, J. G. 1980*a*, *Ap. J.*, **239**, 495.
———. 1980*b*, *Ap. J.*, **240**, 785.
Gascoigne, S. C. B. 1966, *M.N.R.A.S.*, **134**, 59.
———. 1980, in *IAU Symposium No. 85, Star Clusters*, ed. J. E. Hesser (Dordrecht: Reidel) p. 305.
Gascoigne, S. C. B., Norris, J., Bessell, M. S., Hyland, A. R., and Visvanathan, N. 1976, *Ap. J. (Letters)*, **209**, L25.
Hesser, J. E., Hartwick, F. D. A., and Ugarte, P. 1976, *Ap. J. Suppl.*, **32**, 283.
Hodge, P. W. 1960, *Ap. J.*, **131**, 351.
———. 1961, *Ap. J.*, **133**, 413.
Iben, I., Jr. 1981, *Ap. J.*, **246**, 278.
Iben, I. Jr., and Truran, J. W. 1978, *Ap. J.*, **220**, 980.
Lloyd Evans, T. 1980, *M.N.R.A.S.*, **193**, 87.
McGregor, P. J., and Hyland, A. R. 1982, *Ap. J.*, submitted.
Mould, J., and Aaronson, M. 1979, *Ap. J.*, **232**, 421.
———. 1980, *Ap. J.*, **240**, 464.
Persson, S. E., Aaronson, M., and Frogel, J. A. 1977, *A. J.*, **82**, 729.
Rabin, D. M. 1980, Ph.D. thesis, California Institute of Technology.
———. 1982, preprint.
Renzini, A., and Voli, M. 1981, *Astr. Ap.*, **94**, 175.
Richer, H. 1981, *Ap. J.*, **243**, 744.
Searle, L., Wilkinson, A., and Bagnuolo, W. G. 1980, *Ap. J.*, **239**, 803 (SWB).
Struck-Marcell, C., and Tinsley, B. M. 1978, *Ap. J.*, **221**, 562.
Thuan, T. X., and Gunn, J. E. 1976, *Pub. A. S. P.*, **88**, 543.
Tifft, W. G. 1963, *M.N.R.A.S.*, **125**, 199.
van den Bergh, S. 1981, *Astr. Ap.*, **46**, 79.
van den Bergh, S., and Hagen, G. L. 1968, *A.J.*, **73**, 569.
Walker, M. F. 1971, *Ap. J.*, **167**, 1.
———. 1979*a*, *M.N.R.A.S.*, **186**, 767.
———. 1979*b*, *M.N.R.A.S.*, **188**, 735.
Zinn, R. 1980, *Ap. J. Suppl.*, **42**, 19.

Notes added in proof.—(1) We stress that the unambiguous detection of carbon stars in the integrated infrared light of external galaxies will depend upon accurate measurements of the CO band strength. Red broad-band colors in the range $J-H > 0.7$, $H-K > 0.3$ *can* be produced by late-type oxygen-rich stars as well as C stars. (2) Renzini (1981; *Ann. Phys.*, **6**, 87) has discussed the theoretical fraction of the bolometric energy output due to AGB stars in composite systems. His results are consistent with our observational findings. (3) Iben and Renzini (1982 preprint; to appear in *Ann. Rev. Astr. Ap.*, Vol. **21**) have also discussed the differences in the temperatures of the SMC and LMC giant branches.

M. Aaronson: Steward Observatory, University of Arizona, Tucson, AZ 85721

J. G. Cohen: Astronomy Department, 105–24, California Institute of Technology, Pasadena, CA 91125

J. A. Frogel: Cerro Tololo Inter-American Observatory, Casilla 603, La Serena, Chile

K. Matthews: Division of Physics, Mathematics, and Astronomy, 320-47, California Institute of Technology, Pasadena, CA 91125

S. E. Persson: Mount Wilson and Las Campanas Observatories, 813 Santa Barbara Street, Pasadena, CA 91101